1973-12

Digital processing of acoustic signals with application to an ASW signal processor

Adler, Vance Erick

Monterey, California. Naval Postgraduate School

DIGITAL PROCESSING OF ACOUSTIC SIGNALS WITH APPLICATION TO AN ASW SIGNAL PROCESSOR

Vance Erick Adler

NAVAL POSTGRADUATE SCHOOL
Monterey, California

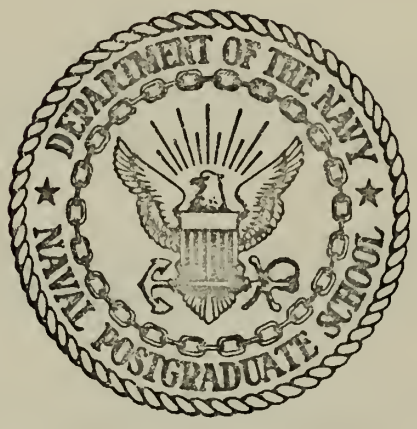

THESIS

DIGITAL PROCESSING OF ACOUSTIC SIGNALS

WITH APPLICATION TO AN

ASW SIGNAL PROCESSOR

by

Vance Erick Adler

Thesis Advisor: G. A. Rahe

December 1973

Digital Processing of Acoustic Signals With Application to an ASW Signal Processor

by

Vance Erick Adler
Lieutenant, United States Navy
B.S., San Jose State College, 1967

Submitted in partial fulfillment of the
requirements for the degree of

MASTER OF SCIENCE IN AERONAUTICAL ENGINEERING

from the

NAVAL POSTGRADUATE SCHOOL
December 1973

ABSTRACT

There is a growing need within the Navy for methods of detecting discrete narrowband signals in a non-stationary background. This paper concerns itself with the application of digital processing and spectral analysis techniques toward that goal. The use of the fast Fourier Transform in estimating the power spectrum of a signal is described. The method involves sectioning the time record, making "raw" estimates of the spectrum from these sections, and averaging these "raw" estimates. It is shown that more stable estimates are available if the segments are overlapped and an optimum amount of overlap for the case of the Hanning Window is found. It is shown that the stability of these spectral estimates can be interpreted as processing gain in the case of a discrete narrowband signal in additive noise. And finally, a brief description of signal detection theory applied to a human observer is presented to emphasize the flexibility that a human operator can bring to a signal detection system.

TABLE OF CONTENTS

I. INTRODUCTION

Today's ASW signal processing systems continue to grow in complexity and while many functions will be automated in systems now under development, the human operator will continue to play a key role in the processing of data and the making of decisions. Man provides a flexibility to the system that is not available through complete automation and it is, therefore, imperative that he be considered an integral part of the system.

In the past, assumptions have been made regarding the requirements that could be imposed upon the operator, without any precise knowledge of how an operator's performance actually would be influenced by the sustained demands of a system. In general, it apparently has been assumed by system designers that the operator was like any of the hardware components that go into a system, i.e. that he would continue to perform at a level throughout a mission approximately equal to that at which he began. Common sense does not support this assumption, but to assume otherwise introduced difficult problems for which no useful answers were available. It seemed wise, or at least expedient, to let the characteristics of the electronics determine the direction of design and the development of procedures for the use of the system, with only casual consideration of the characteristics of the operator. However, studies of the role of the operator indicate that the rate of degradation of operator efficiency, and therefore system effectiveness, is a function of time. And it is much more rapid than even the most critical "user" or the most knowledgeable designer would have thought reasonable when

the systems were much less complicated, and demands on the operator were much less drastic than at present.

The quality of the operator's decision is based, to a great extent, on his insight and understanding of the problem. Thus, the primary objective of a system which utilizes a human observer is to provide the operator with the necessary insight and understanding of the problem to enable him to make the best decision possible. To do this, the display should utilize natural qualities of human perception so as not to drain the operator psychologically or expect him to make dicisions based on information he is not able to fully perceive.

The quality of the operator's decision is also based on the accuracy with which the information provided him actually represents the physical situation. The purpose of the passive ASW processor is to detect the presence of certain narrowband signals with random phase variation from a background of random ocean noise. It has been shown that the optimum receiver, in a maximum likelihood sense, for detection of such signals is an infinite set of Fourier filters followed by incoherent integration integration of power and a decision element (Williams, 1972). The present level of technology indicates that digital processors offer the high resolution, high dynamic range, repeatability, and flexibility necessary to effectively produce such a receiver.

The purpose of this paper is to discuss the digital processing of acoustic signals with application to a new generation of passive ASW signal processors being developed today. Specific mention will be made of techniques in the "Spotlight" processor under development at the Naval Postgraduate School by Professor G.A. Rahe.

General digital processing considerations are discussed. The statistical properties of the spectral estimate are presented as well as methods

for improving them. The processing gain available from a system, which utilizes the FFT as a filtering device and incoherently integrates the power, is derived and finally a brief description of detection theory applied to a human observer in a sequential observation task is discussed.

II. DATA ANALYSIS

A. NOISE REPRESENTATION

The ambient acoustic wave fields in the ocean are often quite energetic and contain a wide range of frequencies. The study of these noise fields forms an important and necessary prelude to any serious design of detection systems. In the ocean, for example, one finds biological noise sources, noises due to wave action at the surface of the water, noises produced by meteorological conditions such as precipitation, and a great deal of shipping noise. For passive detection systems, these noise fields furnish the background out of which signals must be detected. From the experimental work of Parkins (1968) it seems reasonable to assume that the ocean noise field may, at least a large percentage of the time, be modeled as a weakly stationary, Gaussian random process.

In order to understand the theoretical concepts of signal processing it is necessary to characterize the ambient noise field (and the desired signals) in commonly understood mathematical terms. The frequency domain (spectral) representation in which the "signal" is decomposed into a set of sinusoidal components as specific frequencies will be considered here.

Select a particular sample function of noise and select from that sample an interval of duration L extending, say, from $t = -L/2$ to $t = L/2$. Such noise sample $n^{(s)}(t)$ is shown in figure 2.1(a). Now generate a periodic waveform in which the waveform in the selected interval is repeated every L seconds as in figure 2.1(b). This <u>periodic</u> signal $n_L^{(s)}(t)$ with period L can be represented as a sum of harmonically related sinusoids (Fourier series) as follows:

$$n_L^{(s)}(t) = A_o + \sum_{k=1}^{\infty} A_n \cos(2\pi k f_o t - \phi_k) \qquad (2.1)$$

where A_o is a DC level; A_k and ϕ_k are, respectively, the amplitude and phase of each sinusoid (line); and f_o (the fundamental frequency) is 1/L. Plots of A_k and ϕ_k as functions of frequency are referred to as amplitude and phase spectra, respectively. A_k and ϕ_k are given by

$$A_k = \sqrt{a_k^2 + b_k^2} \quad ; k = 1,2,3,... \qquad (2.2)$$

and

$$\phi_k = \tan^{-1}(b_k/a_k) \; ; k = 1,2,3,... \qquad (2.3)$$

where

$$a_k = \frac{2}{L}\int_{-L/2}^{L/2} n_t^{(s)}(t) \cos(2\pi k f_o t)dt \; ; k = 1,2,3,... \qquad (2.4)$$

and

$$b_k = \frac{2}{L}\int_{-L/2}^{L/2} n_t^{(s)}(t) \sin(2\pi k f_o t)dt \; ; k = 1,2,3,... \qquad (2.5)$$

(a_k and b_k are Fourier coefficients). The DC level a_o is obtained by calculating the time average of $n_L^{(s)}(t)$:

$$a_o = A_o = \frac{1}{L}\int_{-L/2}^{L/2} n_L^{(s)}(t)dt \qquad (2.6)$$

Several examples of amplitude and phase spectra of periodic signals are shown in figure 2.2.

Although not all periodic signals can be represented by Fourier harmonic series, the class which can be is large. The limitations of the representation are discussed in Thomas and in Jenkins and Watts. Several other forms of Fourier series are also discussed in the literature. The form of eqn. 2.1 is a modified trigonometric version and is useful from an intuitive standpoint. Another form, which is more convenient for mathematical manipulations, is the exponential or complex version in

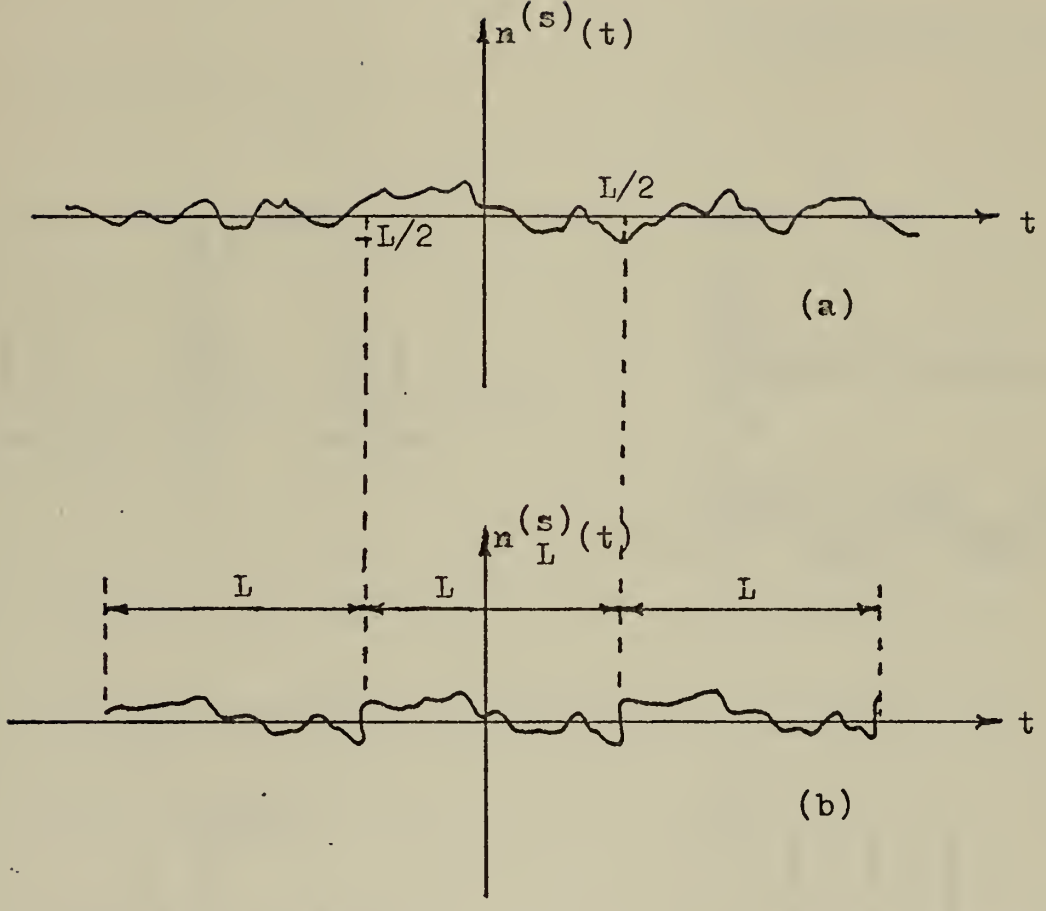

Figure 2.1. (a) A sample noise waveform. (b) A periodic waveform is generated by repeating the interval in (a) from -L/2 to L/2.

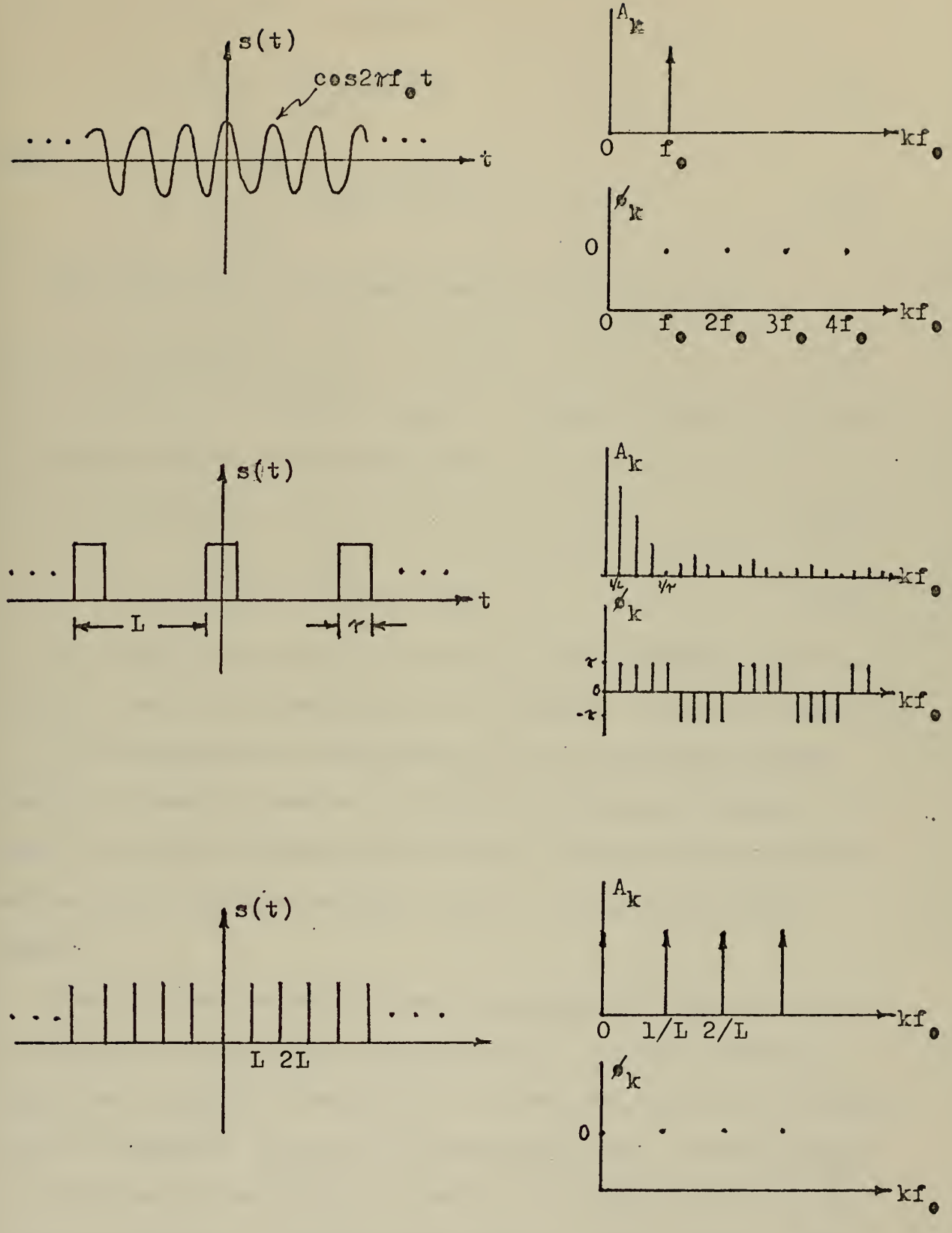

Figure 2.2. Amplitude and phase spectra of some periodic signals.

which the signal $n_L^{(s)}(t)$ is given by

$$n_L^{(s)}(t) = \sum_{k=-\infty}^{\infty} c_k e^{j2\pi k f_o t} \tag{2.7}$$

where

$$C_k = \frac{1}{L} \int_{-L/2}^{L/2} n_L^{(s)}(t) e^{-j2\pi k f_o t} dt \; ; \quad k = 1,2,3,... \tag{2.8}$$

The coefficients C_k are complex and have the property that

$$C_k = C_{-k}^{*} \tag{2.9}$$

(i.e. C_k and C_{-k} are complex conjugates). These coefficients are related to the coefficients in equation 2.1 by

$$C_o = A_o = a_o \tag{2.10}$$

$$C_k = \frac{A_k}{2} e^{j\phi k} = 1/2(a_k + jb_k) \tag{2.11}$$

The exponential spectrum of the Fourier series produces a two-sided spectrum, each of half amplitude, one at frequency f and one at frequency -f. Although equation 2.7 indicates that the representation includes negative frequencies, this is not of physical significance because, in terms of this representation, the sum of the components at the positive and negative frequencies produces a real (in a mathematical sense) quantity.

Frequency domain representations of non-periodic signals require a generalization of the Fourier series approach. One might intuitively reason that L approaches infinity for a nonperiodic signal, which implies that the fundamental frequency (1/L) approaches zero. If this reasoning is carried out mathematically, it leads to a representation of the signal as a continuum of frequencies rather than a "line" spectrum. The continuous representation (Fourier integral or Fourier transform) is

given by

$$n(t) = \int_{-\infty}^{\infty} N(f)e^{j2\pi ft}\, df \tag{2.11}$$

where

$$N(f) = \int_{-\infty}^{\infty} n(t)e^{-j2\pi ft}\, dt \tag{2.12}$$

In general, N(f) is a complex quantity that can be represented by its amplitude and phase components as follows:

$$N(f) = |N(f)|e^{j\phi(f)} \tag{2.12a}$$

Plots of N(f) and $\phi(f)$ as functions of frequency are called amplitude and phase spectra, respectively, and are analogous to the discrete A_k and ϕ_k. Several examples of the amplitude and phase spectra of nonperiodic signals are shown in figure 2.3. Note the similarity between the continuous spectra and the envelope of the line spectra in figure 2.2.

It should be noted, however, that not all time functions possess a Fourier transform. The condition for the existence of the Fourier transform is that the Fourier integral exist in the limit as $T\to\infty$. Existence is guaranteed by absolute convergence of the integral of equation 2.12,

$$\int_{-\infty}^{\infty} |n(t)|^2\, dt < \infty \tag{2.12b}$$

A number of functions having great usefulness do not meet this requirement; functions such as sine waves or step functions. These functions are nevertheless being handled by allowing the Fourier transform to contain impulses. In practice, the class of signals which are Fourier transformable is sufficiently large to encompass a wide variety of applications.

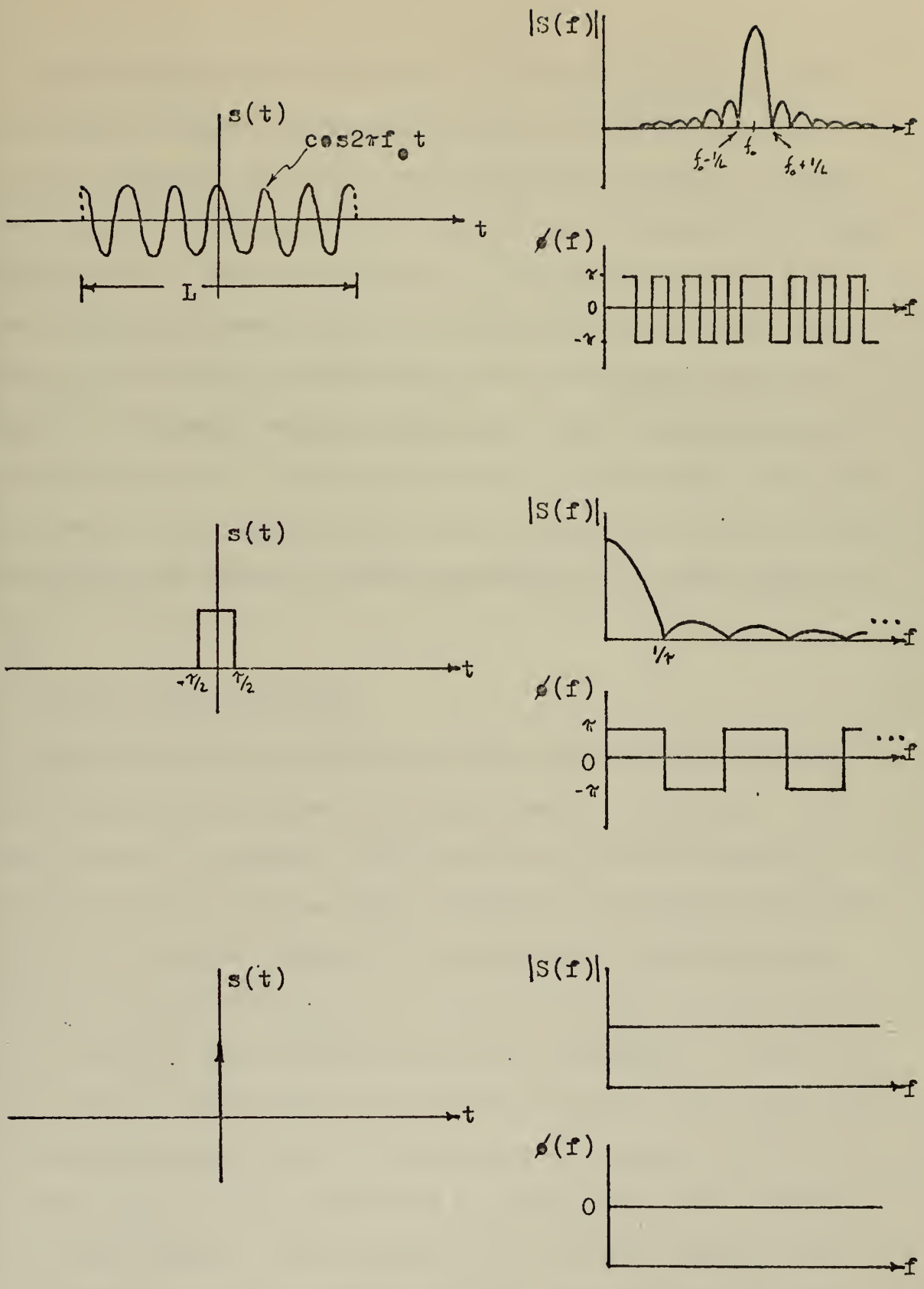

Figure 2.3. Amplitude and phase spectra of some nonperiodic signals.

Fourier series and Fourier transforms of signals differ in their theoretical solutions attributable primarily to the fact that, for practical purposes, only finite length signals can actually be sampled and computed. The results of this computation are used only to provide estimates of the theoretical solutions. As seen in equation 2.7, the series method requires the sum of an infinite number of discrete sinusoids and the integral method requires an infinitesimal frequency resolution. Therefore, only approximations to these representations are obtained in practice. The discrete Fourier Transform (DFT), which will be discussed later, approximates a Fourier series by arbitrarily forcing the signal to be periodic and then truncating it to a finite number of terms.

B. DIGITAL SIGNAL PROCESSING

During the decade of 1960-1970, an important new approach to waveform manipulation, or signal processing, came into importance. It became practical to represent information-bearing waveforms digitally, that is, symbolically, and to do signal processing on the digital representation of the waveform. Thus all the flexibility of digital computers became available for processing of waveforms, and this has had an effect on all fields in which waveform processing is important. It became apparent that one could manipulate waveforms digitally in ways that would be totally impractical with continuous representations. One advantage in this respect is the freedom from time constraints when a waveform is in a digital memory. Once a waveform is in a computer memory, it may be considered to have any desired time base associated with it. As a result of the Fast Fourier Transform (FFT) algorithm, it became practical to do signal processing on waveforms in either the time or the frequency

domain, something never practical with continuous systems. The Fourier transform became not just a theoretical discription, but a tool; and real-time digital spectral analysis became a reality. Some of the practical considerations of performing this processing will be discussed in this section.

1. Sampling Considerations

Digital signal processing is based on the principle that an analog signal can be represented by the values of the signal at discrete points in time. This principle is embodied in the sampling theorem, which states that a band-limited signal is completely characterized by a set of samples taken at a minimum rate of $2f_{max}$ (called the Nyquist rate), where f_{max} represents the highest frequency component in the signal. Although this statement of the sampling theorem appears straightforward, there are several practical considerations which should be discussed.

One difficulty in applying the sampling theorem is that actual signals do not occupy well defined frequency bands, i.e., the spectra of real signals tend to gradually roll off until the amplitude of the spectral components reaches a minimum detectable level. Therefore, most sampling systems have a filter just before the quantizing device to limit the signal to a predetermined band. This filter is called an anti-aliasing filter.

When analog data are quantized i.e., converted from a continuous waveform to discrete values, at a rate of f_s samples per second, the analog spectrum is divided into frequency bands of width $f_s/2$ (figure 2.4a). During sampling, the energy in each band is folded or aliased into the lowest band (0 to $f_s/2$) and $f_s/2$ is called the folding frequency. The

folding operation can be envisioned if the bands in figure 2.4a are viewed from "above", as in figure 2.4b. The original analog spectrum is collapsed into the lowest frequency band, and the even-numbered bands are inverted in frequency as they are folded. Therefore, the net result of the sampling process is that, in spectra computed from the digital samples, all energy in the original analog spectrum appears in the band 0 to $f_s/2$ as seen in figure 2.4c. Figure 2.5a shows an example of a typical aliasing situation. It is obvious that the spectrum computed from the digital samples (figure 2.5b) provides very little information concerning the actual frequency content of the original signal because the original location of the computed spectral components is unknown. Only by containing the original spectrum in a single known band can the frequency content be unambiguously determined.

Typically we think of two types of antialiasing filters, the low-pass filter and the band-pass filter. Both have application in digital signal processing and will be briefly discussed here.

The low-pass anti-aliasing filter will be assumed to have a frequency response function as shown in figure 2.6. The amplitude level of the aliased components is given by

$$A_a = M_h \frac{\log_{10}(f_s - f_h) - \log_{10} f_h}{\log_{10} 2} \tag{2.13}$$

$$= 3.32\, M_h \log_{10}(f_s/f_h - 1) \quad \text{db} \tag{2.14}$$

where f_s is the sampling frequency, f_h is the filter cutoff frequency, and M_h is the filter rolloff slope (db/octave). Equation 2.14 applies when the original analog signal spectrum is assumed to have components at frequencies that are above the folding frequency and equal in amplitude to components in the pass band.

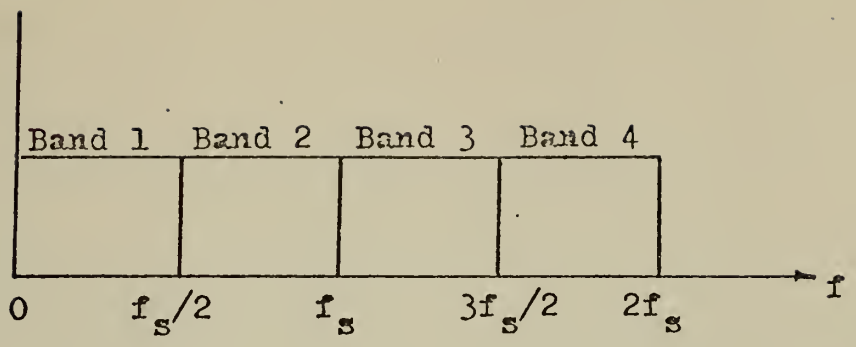

(a) Effect of sampling the original analog spectrum

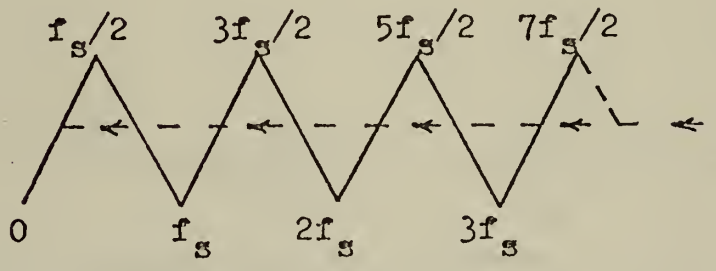

(b) Folding operation viewed from "above".

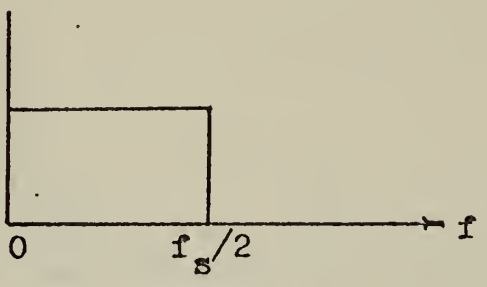

(c) Bandwidth of the spectrum computed from the digital samples.

Figure 2.4. Aliasing effect of sampling on the Fourier spectrum.

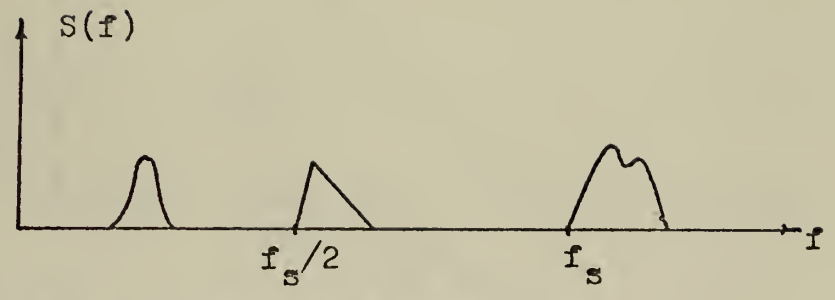

(a) Original analog spectrum

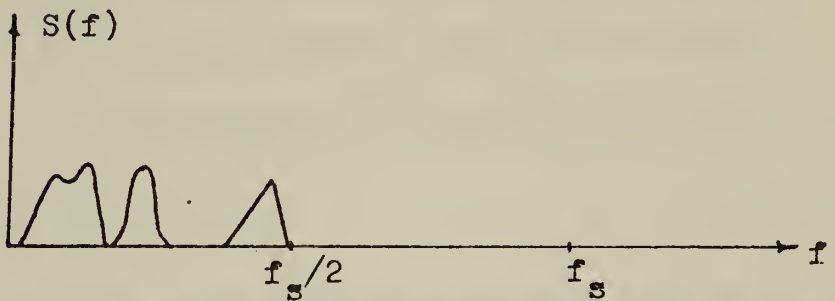

(b) Spectrum computed from digital samples

Figure 2.5. Typical antialiasing situation

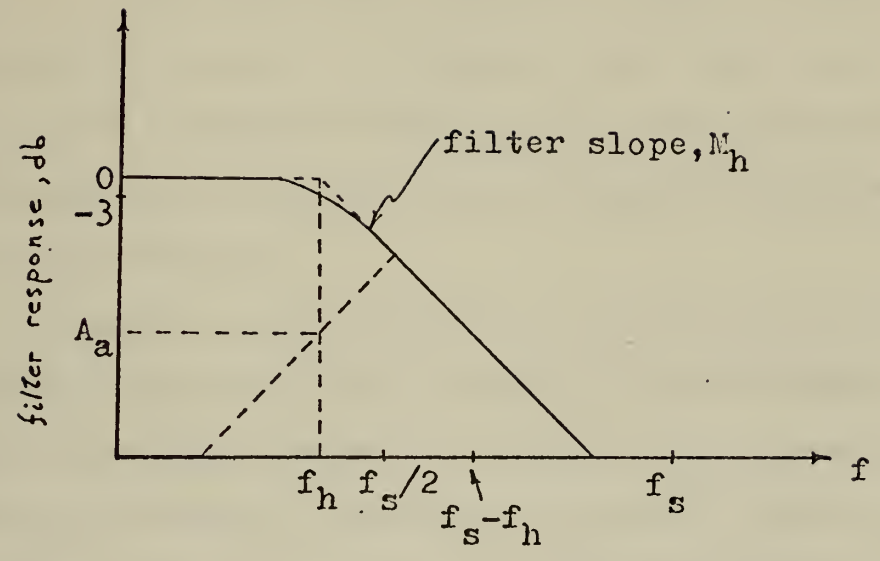

f_s= sampling frequency

f_h= filter cutoff frequency(-3 db)

M_h= filter rolloff slope(db/octave)

A_a= amplitude of aliased component

Figure 2.6. Low-pass antialiasing filter

High-quality variable-cutoff commercially available filters generally have rolloff slopes from -12 to -48 db/octave. Sample frequencies usually are approximately three to four times the filter cutoff frequency and in order to provide a margin of safety from aliasing effects, an anti-aliasing filter slope of at least -36 db/octave and preferrably -48 db/octave are desirable. These figures apply to situations in which a variety of general-purpose signal processing techniques will be applicable. Less conservative parameters can be substituted as the situation dictates.

A bandpass signal of bandwidth W and center frequency f_c can be sampled at a rate greater than or equal to twice the bandwidth rather than twice the highest frequency component, if appropriate antialiasing filtering is performed. The bandpass antialiasing filter will be assumed to have the frequency response function shown in figure 2.8. Once the sample frequency has been chosen, the level of the components aliased from above the band of interest (assuming they are equal in amplitude to the passband components) is given by

$$A_{sh} = 3.32\ M_h \log_{10}(K\ f_s/f_h - 1) \quad \text{db} \tag{2.15}$$

where f_h is the upper filter cutoff frequency, M_h is the filter slope (db/octave), f_s is the sample frequency, and K is the band number (see figure 2.7). The level of the components aliased from below the band of interest is given by

$$A_{s\ell} = -3.32\ M_\ell \log_{10}[(K-1)f_s/f_\ell - 1] \quad \text{db} \tag{2.16}$$

where f_ℓ and M_ℓ are the lower filter cutoff and slope, respectively.

The procedure for choosing the sample frequency in bandpass situations is not as straightforward as in the low-pass case. However, a fairly simple iterative procedure is as follows.

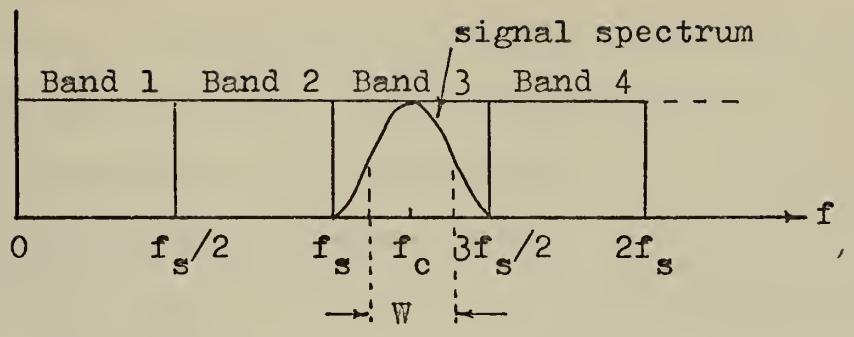

Figure 2.7. Sampling of a bandpass signal

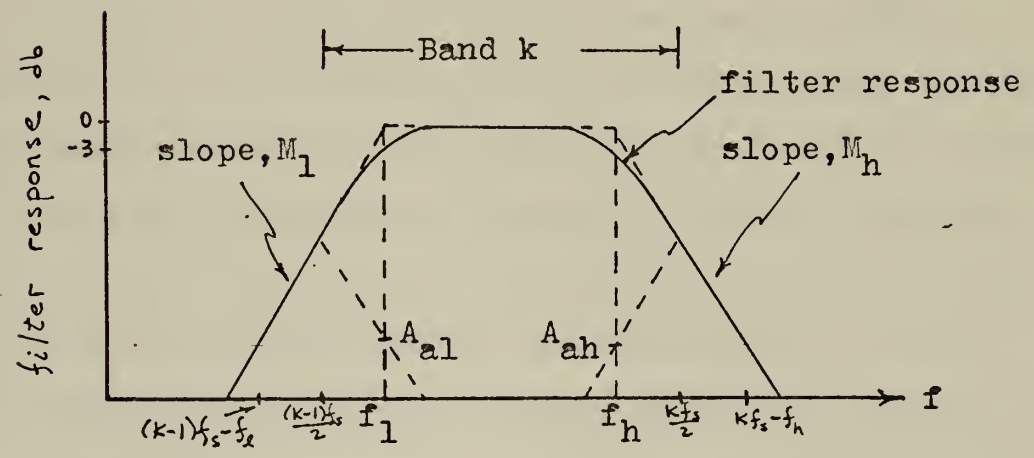

Figure 2.8. Bandpass antialiasing filter

1. Define an effective signal bandwidth W' that is about two to four times the actual bandwidth of interest, depending on the steepness of the filter rolloff.

2. Select a sampling band by choosing K to be the largest integer such that $K < f_c/W' + 1/2$. This will guarantee that the signal band W' will be encompassed by a sampling band.

3. Define the sample frequency to be

$$f_s = \frac{2f_c}{K-1/2} \tag{2.17}$$

4. Calculate values for A_{sh} and $A_{s\ell}$. If these values are not acceptable, repeat steps 1 through 4 using a larger effective bandwidth W'.

5. If it is inconvenient to generate the exact sample frequency calculated in eq. 2.17, it may be adjusted as needed. Recalculation of A_{sh} and $A_{s\ell}$ will indicate if a significant amount of aliasing will result from the adjustment.

The effect of sampling properly filtered bandpass signals at a rate proportional to the bandwidth is the bandshift the signal spectrum to the baseband (figure 2.4c). This means that when spectra are computed with digital samples the frequency axis must be labeled in accordance with the location of the original signal spectrum. This location is a function of the sampling band number K and sample rate f_s. For odd-numbered bands, the frequency axis should be labeled from $(K-1)f_s/2$ to $kf_s/2$ as shown in figure 2.9a. For even-numbered bands, the scale runs from Kf_s to $Kf_s/2$ (figure 2.9b). Note that in the even-numbered bands, it is desirable to rotate the plot about the vertical axis and translate the frequency axis such that it runs from $Kf_s/2$ to Kf_s.

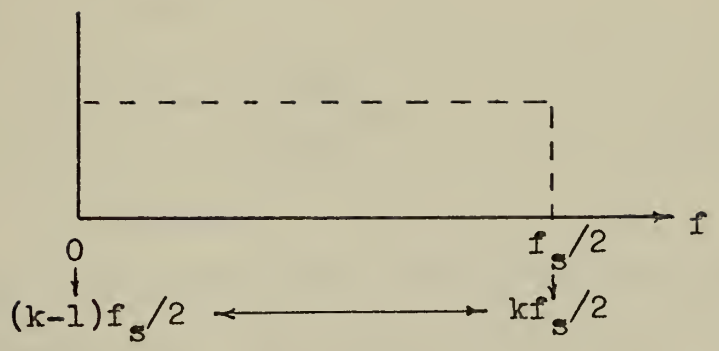

(a) k odd

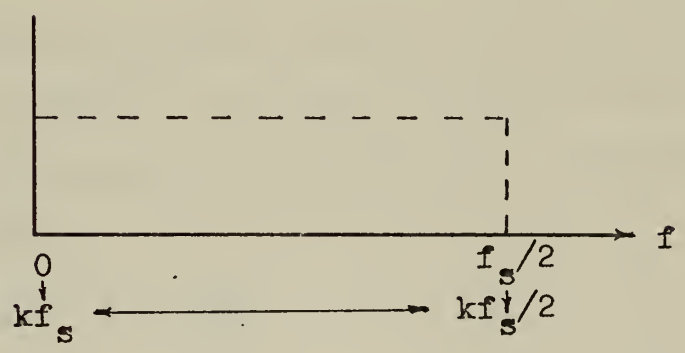

(b) k even

Figure 2.9. Relabeling of frequency axis of computed spectra

2. Dynamic Range and Quantization Error

The dynamic range of an analog-to-digital (A/D) converter can be defined as the ratio between the maximum and minimum peak signal values or as the signal-to-quantization noise ratio, depending on the usage of the digital samples. The maximum peak signal range in db (figure 2.10) is given by

$$D = 20 \log_{10} \frac{V_{max}}{V_{max}/2^{n-1}} \tag{2.18}$$

$$= 6.02(n-1) \tag{2.19}$$

where V_{max} is the maximum input voltage level and n is the number of bits (including sign) of the bipolar A/D converter. For example, a 12-bit bipolar A/D converter has a peak signal range of about 66 db, which is compatable with most analog instrumentation devices, e.g., tape recorders.

Quantization noise is caused by the stepwise approximation of the digital samples to the original continuous signal and can be treated as an additive noise component (figure 2.10). The RMS quantization noise is given by

$$N_Q = 0.29 \frac{V_{max}}{2^{n-1}} \tag{2.20}$$

The RMS signal-to-quantization noise ratio (assuming a sine wave of peak amplitude V_{max}) in db is given by

$$SN_Q = 20 \log_{10} \frac{V_{max}/\sqrt{2}}{.29\ V_{max}/2^{n-1}} \tag{2.21}$$

$$= 20 \log_{10} \frac{2^{n-1}}{.41} \tag{2.22}$$

$$= 20 \log_{10} 2^{n-1} + 7.74 \tag{2.23}$$

$$\simeq D + 8 \tag{2.24}$$

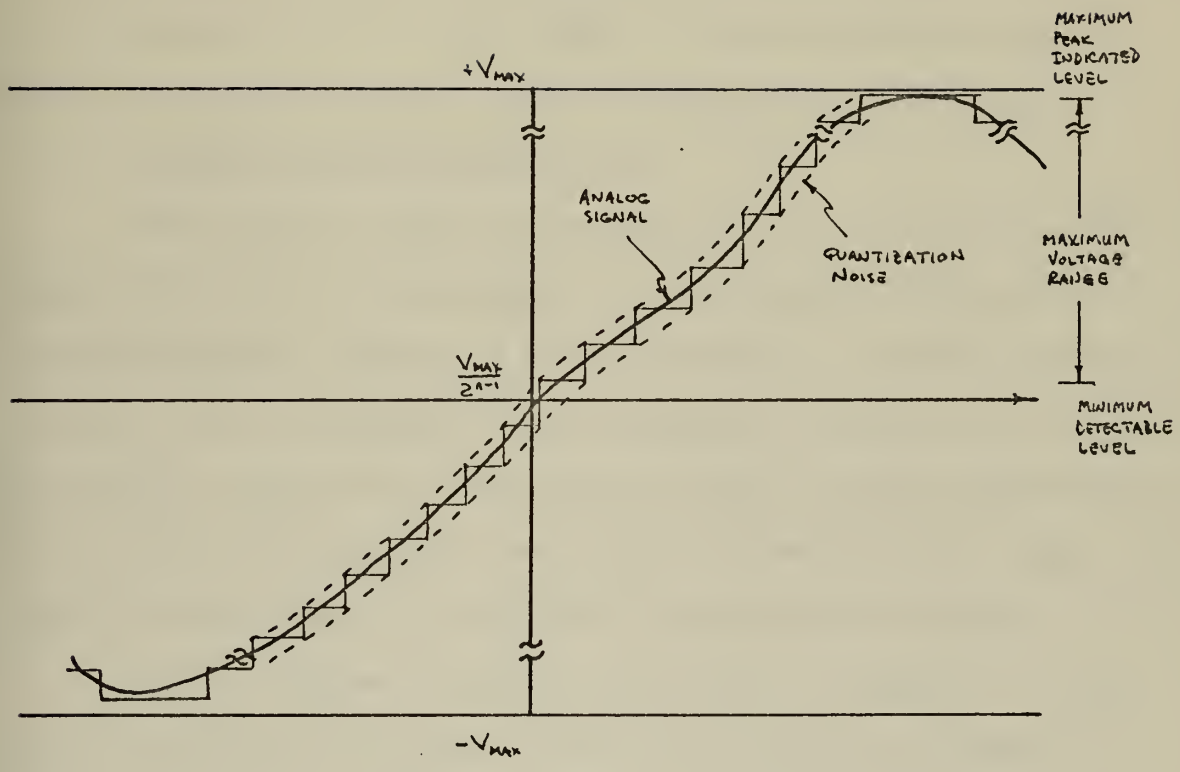

Figure 2.10. Effects of quantizing an analog signal

Therefore, a 12-bit bipolar A/D converter will have a signal-to-quantization noise ratio of about 74 db.

Eqs. 2.19 and 2.24 both yield optimistic numbers, i.e., it is usually not possible to sufficiently control the amplitude of the input signal to the A/D converter so that the full voltage range is used. This means that the dynamic range can be reduced by 3 to 6 db, depending on the variability of the input signal. A buffer amplifier prior to the A/D converter is usually needed to condition the signal level.

3. Discrete Fourier Transform (DFT)

When analyzing signals whose parameters are known within broad limits, one of the first operations to be performed is some type of spectral analysis. This can be a single analysis, a series of analyses to indicate the time dependence of the spectral components, or an averaged spectral computation to approximate a power spectral density function. This section discusses some of the considerations for using digital Fourier Transform techniques to analyze sampled signals.

The DFT computes a finite Fourier series to represent a signal over a pre-defined time interval. The time interval L is chosen to include as much of the original signal as desired (figure 2.11a). The DFT, since it is a representation applicable to periodic signals, treats the signal as if it were periodic with period L (figure 2.11b). The discontinuities which may appear because of this forced periodicity are included in the representation and are of primary concern when performing DFT analyses.

The DFT representation is closely analogous to the frequency domain representation for periodic signals (eqs. 2.1 through 2.6); however, it is necessary to express the mathematical operations in terms of

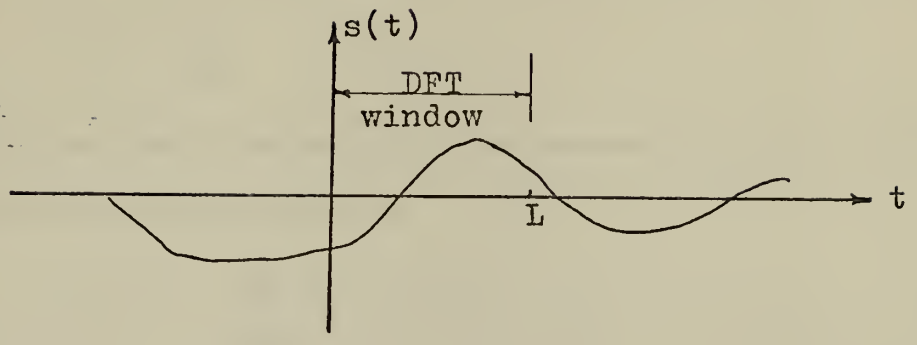

(a) Signal truncation

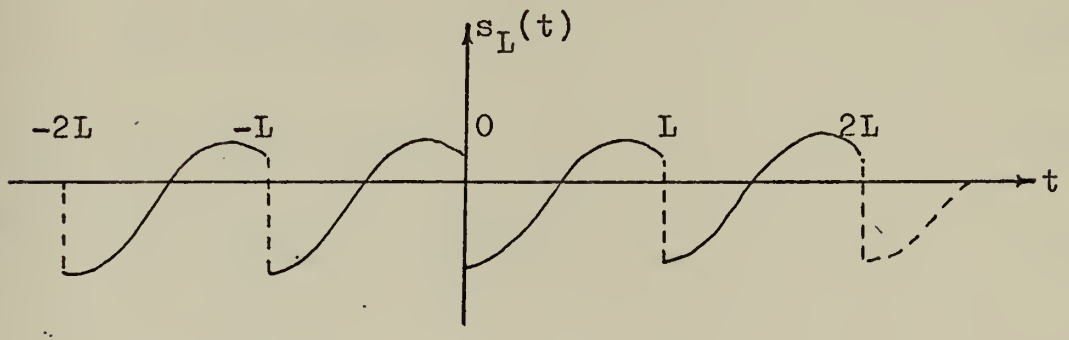

(b) Assumed periodicity

Figure 2.11. DFT processing

sampled signal values. It will be assumed that the signal to be represented or analyzed consists of a set of N equally spaced samples over the time interval L as follows:

$$s(t_i) = s(i \cdot \Delta t) \qquad i = 0,1,2,\ldots,N-1 \tag{2.25}$$

where Δt is the time between samples. The sample spacing is given by

$$\Delta t = \frac{L}{N} = \frac{1}{f_s} \tag{2.26}$$

where f_s is the sample frequency. The representation of the original signal s(t) over the interval L is

$$s(t) = \hat{A}_o + \sum_{n=1}^{N-1} \hat{A}_n \cos(2\pi n \Delta f t + \theta_n) \; ; \; 0 \leq t \leq L \tag{2.27}$$

where

$$\Delta f = 1/L \tag{2.28}$$

the fundamental frequency or "bin" spacing. The amplitude and phase spectra are

$$\hat{A}_n = \sqrt{\hat{a}_n^{\,2} + \hat{b}_n^{\,2}} \tag{2.29}$$

$$\hat{\theta}_n = -\mathrm{Tan}^{-1}(\hat{b}_n / \hat{a}_n) \tag{2.30}$$

where

$$\hat{a}_n = \frac{2}{N} \sum_{i=1}^{N-1} s(t_i) \cos(2\pi n \Delta f t_i) \; ; \; n = 1,2,\ldots,N-1 \tag{2.31}$$

$$\hat{b}_n = \frac{2}{N} \sum_{i=1}^{N-1} s(t_i) \sin(2\pi n \Delta f t_i) \; ; \; n = 1,2,\ldots,N-1 \tag{2.32}$$

The DC term $\hat{A}_o$ is

$$\hat{a}_o = \hat{A}_o = \frac{1}{N} \sum_{i=0}^{N-1} s(t_i)$$

The terms $\hat{a}_n$ and $\hat{b}_n$ are commonly called the real and imaginary Fourier coefficients, respectively.

When the signal to be analyzed by DFT methods is real, the amplitude and phase spectra have certain symmetrical properties. Mathematically, the symmetry is given by

$$\hat{A}_{(N/2)+(i-1/2)} = \hat{A}_{(N/2)-(i-1/2)} \; ; \; i = 1,2,\ldots,N/2 \qquad (2.34)$$

which states that the amplitude spectrum has even symmetry about the point (N-1)/2. The phase spectrum exhibits odd symmetry about the point (N-1)/2. i.e.

$$\hat{\theta}_{(N/2)-(i-1/2)} = \hat{\theta}_{(N/2)+(i-1/2)} \; ; \; i = 1,2,\ldots,N/2 \qquad (2.35)$$

In terms of frequency, the point (N-1)/2 can be expressed as $f_s/2$, the folding frequency. The portion of the computed spectrum between (N-1)/2 and N-1 can be treated as the negative half of the spectrum which would normally occupy the band -(N-1)/2 to 0. For real signals, only the values between 0 and (N/2)-1 must be considered.

Signal truncation introduces broadband leakage into the computed spectra, i.e. seemingly narrowband signals will appear to occupy more bandwidth than expected. Severe discontinuities in the pseudoperiodic signal may be present, depending on the relationship of the signal frequencies to the length of the period L (see figure 2.11). This can most easily be illustrated for the case of a sinusoidal signal. If the signal frequency f_c is such that

$$f_c = K\Delta f \; ; \; K = 1,2,\ldots,(N/2)-1 \qquad (2.36)$$

(f_c is harmonically related to Δf) the computed amplitude spectrum will consist of a single line component (figure 2.12a). If the signal frequency is offset by the amount $\Delta f/2$, the spectrum shown in figure 2.12b is obtained. The apparent spectral width of this signal depends more on the truncation effects of the DFT calculation than on the actual signal

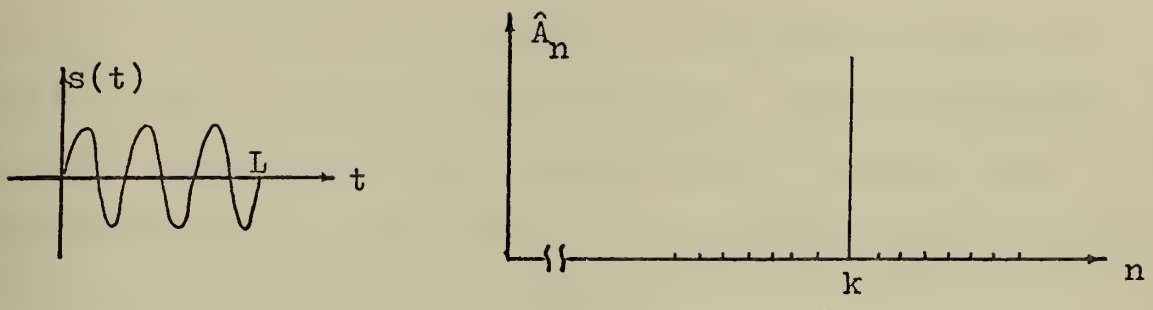

(a) Sine wave harmonically related to Δf

(b) Sine wave midway between two DFT frequency bins

Figure 2.12. DFT amplitude spectra

bandwidth. The solution to this problem is to apply a "smoothing" window to the input data to eliminate or minimize the discontinuities. Windowing functions will be discussed in the next section.

Although the subtleties of the DFT implementations are beyond the scope of this discussion, there are some implementation considerations with which the analyst must be acquainted. Until several years ago, spectrum analysis by digital techniques was an extremely time-consuming process, i.e., computation times proportional to N^2, where N is the number of points in the transform.

Presently, most DFT calculations are performed with fast Fourier transform (FFT) algorithms which have computation times proportional to $N \log_2 N$ (N is assumed to be a power of 2). The FFT has made it possible to perform digital spectral analysis calculations in reasonable lengths of time, making on-line digital spectral analyzers a reality. However, at least in small computer systems, these algorithms are generally implemented in fixed point arithmetic which is subject to overflow. Thus, considerable care must be taken to properly scale the FFT computations, especially in situations where the signal energy falls into a small number of frequency bins.

These overflows are particularly troublesome because they generally appear as spurious components at unpredictable frequencies. The best way to prevent overflow while still maintaining the dynamic amplitude range of the calculation if to perform dynamic scaling on intermediate computed values in the algorithm. All scaling factors should be stored in a way that will permit the computed output values to be calibrated with respect to the known input voltages. Experience indicates that this type of scaling, along with appropriate windowing,

provides a dynamic range (ratio of the peak spectral component to the computational noise floor) of at least 80 db when implemented on a computer with 16-bit words.

4. Window Functions

In practice it is only possible to obtain finite lengths of records. The statistical questions to be considered later stem from the fact that it is necessary to estimate the accuracy of various functions obtained from finite amounts of data. From the preceding discussion on truncation effects and spectral leakage, it should be clear that the operation for taking a finite length record is equivalent to multiplying the actual signal s(t) by the data window w(t). The DFT actually uses samples from the function s'(t), which is given by

$$s'(t) = w(t)\, s(t) \tag{2.37}$$

where s(t) is the original signal and w(t) is zero everywhere but on the interval 0 to L. In the frequency domain, eq. 2.37 becomes

$$s_L(f) = w(f) * s(f) \tag{2.38}$$

$$= \int_{-\infty}^{\infty} S(g)W(f-g)\,dg \tag{2.39}$$

where * denotes convolution. This means the actual spectrum of s(t) is convolved with the Fourier Transform of the window function w(t). The DFT, in effect, samples this result at integral multiples of 1/L. Therefore, the shape of the window function's spectrum determines the degree of spectral spreading when a narrowband signal is truncated.

Any reasonable data window w(t) will produce a spectral window W(f) which is concentrated about f=0 but with side lobes which damp out as f gets further away from zero. For small L, $S_L(f)$ may give a very distorted picture of S(f) since the window W(f-g) will be wide and hence

values of S(g) far removed from g = f will contribute to $S_L(f)$ in the integral. As L becomes large the distortion will be reduced. Finally, as L tends to infinity, the transform component at frequency f can be fully determined, since data windows will tend to the generalized function δ as L tends to infinity. Hence, as L tends to infinity, W(f-g) tends to a delta function centered at g = f and so $S_L(f)$ tends to S(f). In reality, of course, this ideal situation is impossible since we are always dealing with finite-length records.

Although there are many different window functions in the literature, the advantages of windowing the data may be adequately observed by noting the differences between the rectangular window (i.e. simply truncating the data) and the Hanning (Cosine) window. It should be noted, however, that the application of any data window is simply a tradeoff between the bandwidth of the main lobe and the attenuation of the side lobes (i.e. a spectral window with a narrow main lobe will have as slower rate of attenuation of the side lobes than a window with a wider main lobe). This comparison can be seen for the rectangular window and the Hanning window in the next two sections.

a. Rectangular Window

The rectangular window is applicable when samples of the original signal are used directly by the DFT. This function is given by

$$W(t) = \begin{cases} 1 & 0 \leq t \leq L \\ 0 & \text{elsewhere} \end{cases} \tag{2.40}$$

(see figure 2.13a). The Fourier transform of w(t) is

$$W(f) = Le^{j2\pi fL} \frac{\sin \pi fL}{\pi fL} \tag{2.41}$$

(see figure 2.13b and c). The actual location of the sin x/x function, and hence the amounts of energy leakage, in relation to the DFT frequency

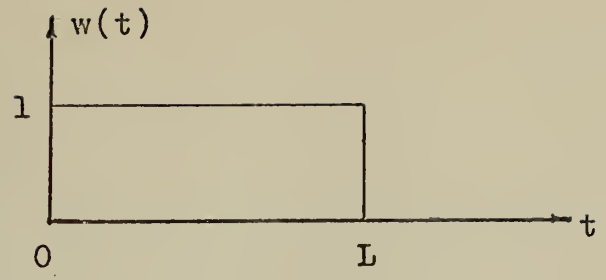

(a) Time domain

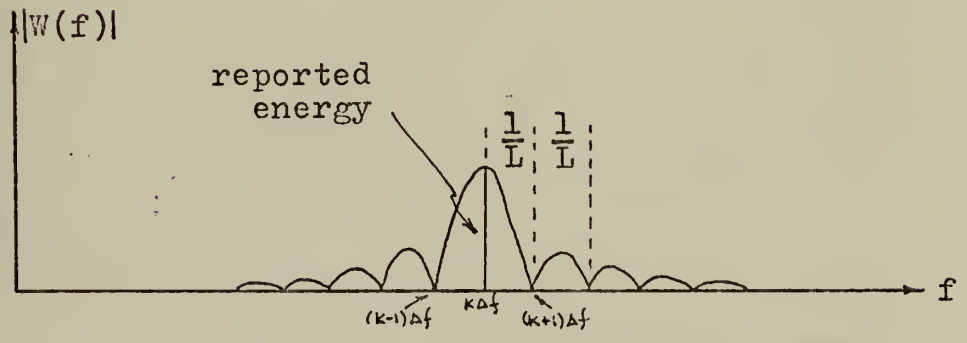

(b) Frequency domain with input signal harmonically related to 1/L.

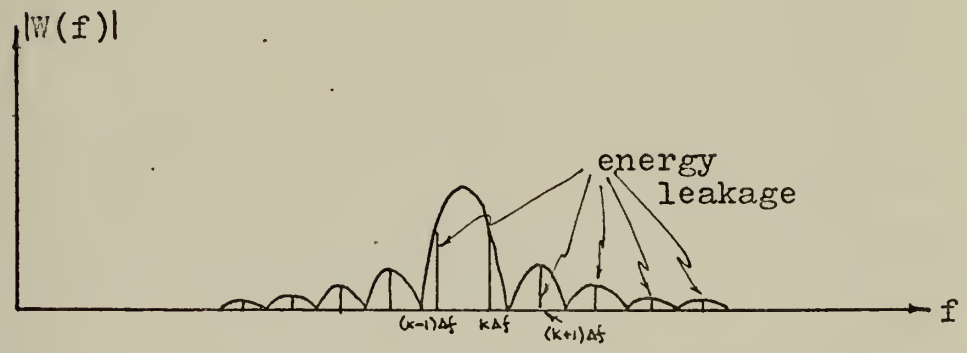

(c) Frequency domain with input signal half-way between two bins.

Figure 2.13. Rectangular window

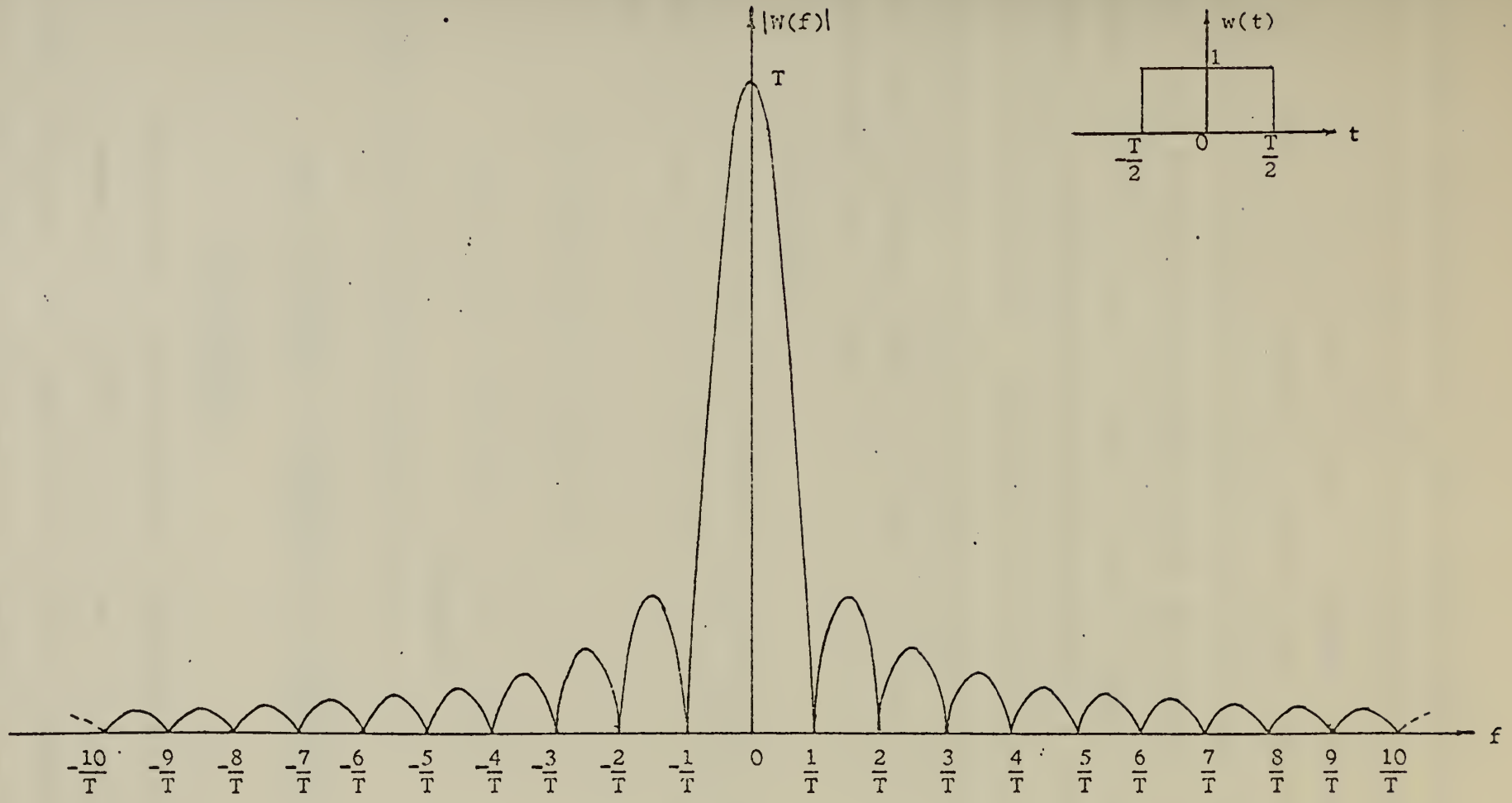

Figure 2.14: Rectangular Window

bins, depends on the frequency of the input signal to which the window is applied. For an input signal frequency which is harmonically related to Δf, the sin x/x function is sampled as shown in figure 2.13b and all signal energy plus any other energy which might be present (noise) under the main and side lobes is reported as being present at the input signal frequency. For a signal frequency halfway between the two bins, the sin x/x function is sampled as shown in figure 2.13c and the signal energy is attenuated and spread throughout all the side-lobes giving a very distorted picture of the actual signal. The relative size of the side-lobe area compared with the main lobe area is very important when considering the amount of energy leakage. Figure 2.14 shows the spectrum of the rectangular-time window drawn to scale.

b. Hanning Window

The Hanning Window is adequate for general-purpose spectral analysis and is easily applied to data either in the time or frequency domain.

The Hanning Window is defined by

$$W(t) = \begin{cases} 1/2(1 + \cos \frac{2\pi t}{t}) & -L/2 \leq t \leq L/2 \\ 0 & \text{Elsewhere} \end{cases} \qquad (2.42)$$

(see figure 2.15). The Fourier Transform of W(t) is

$$W(f) = \frac{L}{2}\left\langle \frac{\sin \pi fL}{\pi fL} + \frac{1}{2}\frac{\sin(\pi fL-\pi)}{(\pi fL-\pi)} + \frac{1}{2}\frac{\sin(\pi fL+\pi)}{(\pi fL+\pi)} \right\rangle \qquad (2.43)$$

$$= \frac{L}{2}\frac{\sin \pi fL}{\pi fL(1-f^2L^2)}$$

From equation 2.43 it is seen that the Hanning Window turns out to be the summation of three sin x/x functions. Since the main lobes are spaced 1/L Hz apart, this window has the effect of averaging three adjacent lobes, giving the center one twice as much weight as the side

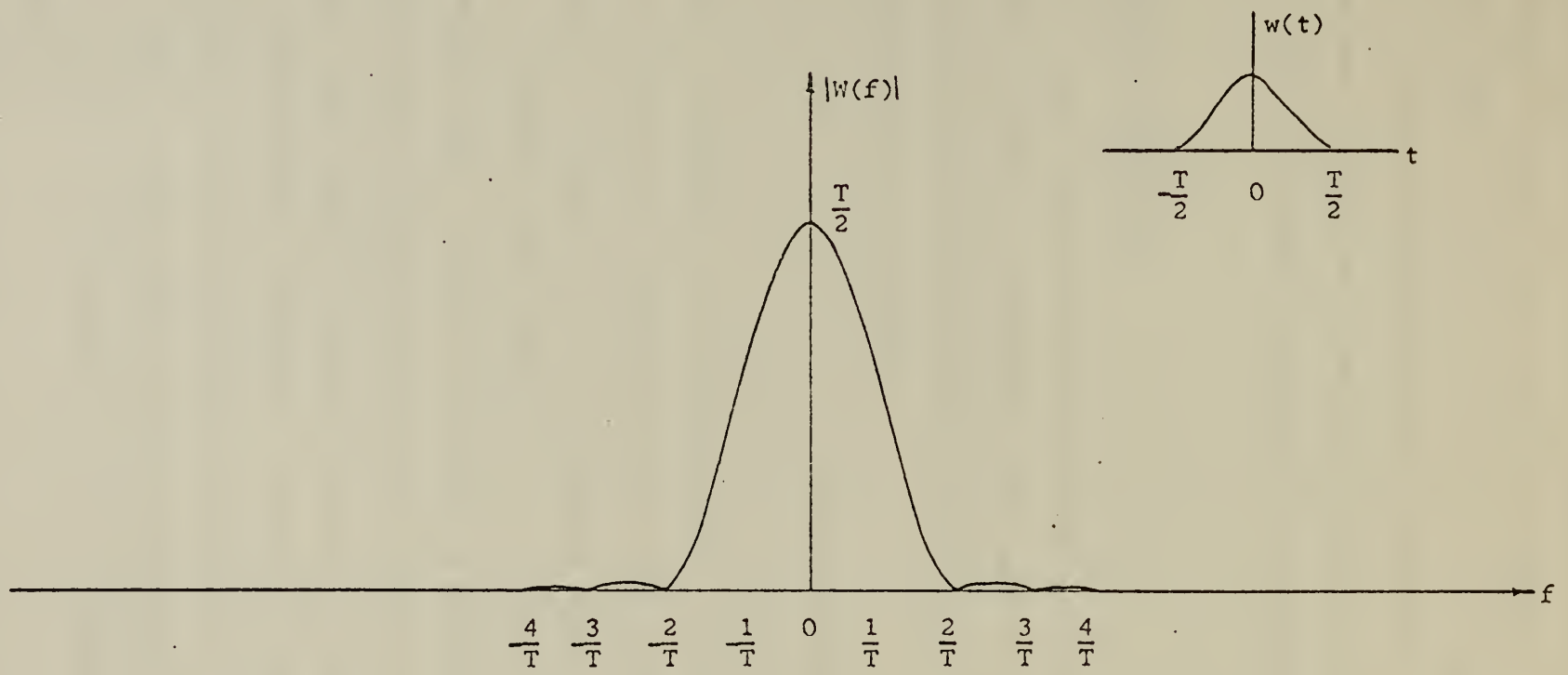

Figure 2.15. Hanning Window

ones. Thus, there will be a tendency to greatly decrease the size of the side lobes. The main lobe is reduced to one-half of its previous value and its width is doubled. The reduction in leakage, therefore, results in a corresponding widening of the bandwidth of analysis. The distance between the first zero crossing on either side of the main lobe is 2/L Hz. Figure 2.15 shows the spectrum of the Hanning window drawn to scale.

C. PROCESSING OF REAL DATA

To see how some of the ideas presented thus far are applied to real data, consider the method of processing being used in the new "SPOTLIGHT" acoustic signal processor being developed by Prof. G. A. Rahe at the Naval Postgraduate School, Monterey.

The idea behind the processor is to present the observer with a continually updated history of the spectrum of the incoming signal and to allow him to interpret the data appropriately. The display of the spectrum is presented as a three-dimensional random surface on a CRT screen as shown in figure 2.16. Each successive update of the display represents an estimate of the incoming signal's spectrum over a length of time T seconds long. As each new estimate is presented, the oldest one is dropped off the back of the display and a new one appears on the front end. Each spectral estimate is formed as follows:

1. A data window w of duration L seconds is applied successively to the available data in the overlapping intervals (0,L), (S,S+L),... [(P-1)S,T], where S is the amount of shift each adjacent data window undergoes, and P is the total number of pieces or segments employed (see figure 2.17).

2. A DFT is performed on each of the P windowed sections using an FFT algorithm and a raw estimate is computed as the magnitude squared of the DFT.

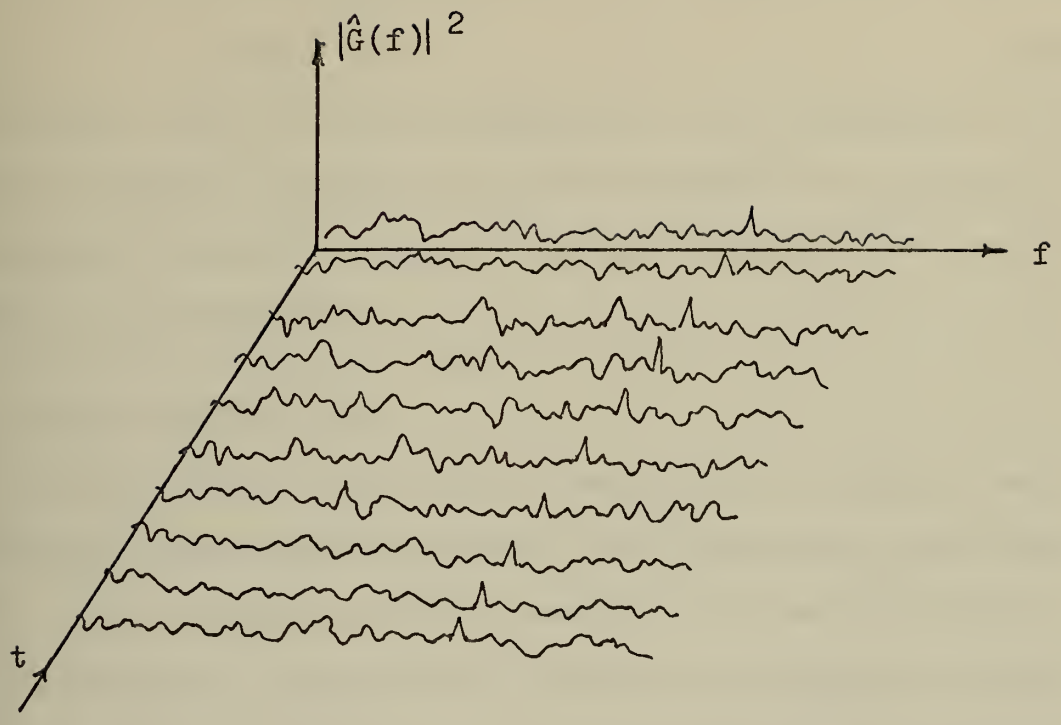

Figure 2.16. "SPOTLIGHT" processor display

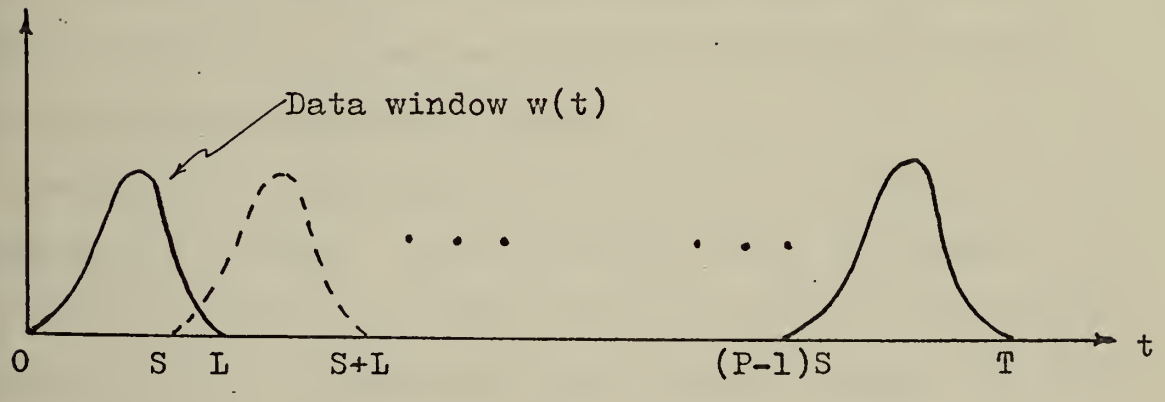

Figure 2.17. Overlapped data windows

3. The smoothed estimate is computed as the average of the P raw estiamtes.

Since L seconds of data are used for each estimate we see that

$$(P-1)S + L = T \tag{2.44}$$

Each estimate need not and most probably will not be independent of the previous estimate. The update rate of the estimates is a function of the operator's needs. The choice of the parameters L, T, and S is discussed in the next section.

D. PRACTICAL CONSIDERATIONS

The effectiveness of the processor depends on its ability to make consistently stable spectral estimated using intelligently chosen paramaters. Some of the more practical aspects of the spectral estimate are now discussed. The parameters associated with making the estimates must necessarily be chosen prior to the processing of any data and should be made to meet certain specifications.

The sampling rate must be chosen so that the spectrum can be estimated in the frequency range of interest, $0 \leq f \leq f_1$. Hence, the sampling rate must be at least $2f_1$. Care must be taken to avoid aliasing as was discussed in section IIB. This is usually done with an anti-aliasing filter prior to sampling the signal so that the power above f_1 in the spectrum is effectively removed.

Associated with reproducing the fine details of the spectrum is the fidelity of the estimate. To achieve high fidelity, the "Bandwidth" of the window used must be of the same order as the width of the narrowest important detail in the spectrum. It is, therefore, useful to be able to make an intelligent estimate as to the width of the smallest important detail required by the system to be "detected". For example, if

the width of the narrowest important detail in the spectrum is known to be .15 Hz, then as spectral window whose "bandwidth" is of the order of .15 Hz or smaller must be used to be able to resolve the fine details of the spectrum. Note that to resolve a spectrum to the same amount of detail, more data (a larger transform) would be required if using the Hanning window than if using the rectangular window since the "bandwidth" of the Hanning window is greater than that for the rectangular window (see figures 2.14 and 2.15). Assuming that the hardware is available, one should not be lulled into ignoring the above considerations and using the finest resolution available, because the requirements for high fidelity and high stability (to be discussed next) are conflicting and any practical realization is necessarily a compromise between the two.

It seems appropriate at this time to say that the frequency "bandwidth" of a narrow band-pass filter (window) is described in several different ways. Three of the most common descriptions for bandwidth which are of interest to the power spectral density measurement are briefly described here.

1. The half-power point bandwidth B_r is defined as

$$B_r = f_2 - f_1 \tag{2.45}$$

where

$$|W(f_1)|^2 = |W(f_2)|^2 = 1/2\ |W_m|^2 \ .$$

B_r is the frequency interval between the upper and lower frequencies where the filter attenuates an applied signal 3 db below maximum transmissibility. This description of bandwidth is convenient because it is easy to measure, but is otherwise of little physical significance for random signal applications.

2. The noise bandwidth B_n is defined as

$$B_n = \frac{\int_0^\infty |W(f)|^2 \, df}{|W_m|^2} \tag{2.46}$$

is the bandwidth of a hypothetical rectangular filter which would pass a signal with the same mean square value as the actual filter when the input is white noise. B_n is a convenient measure of bandwidth to use for normalizing narrowband mean square value measurements, as required for analog power spectral density measurements.

3. The equivalent statistical bandwidth B_s defined as

$$B_s = \frac{\left[\int_0^\infty |W(f)|^2 \, df\right]^2}{\int_0^\infty |W(f)|^4 \, df} \tag{2.47}$$

is the bandwidth of a hypothetical rectangular filter which would pass a signal with the same mean square value statistical error as the actual filter when the input is white noise. In other words, B_s is the description of filter bandwidth which is technically appropriate when considering the statistical error ε of a properly resolved power-spectral density measurement as given by

$$\varepsilon = \frac{1}{\sqrt{B_e T}} \tag{2.48}$$

For the case of an ideal filter, the three descriptions of bandwidth are all equal. For any other filter characteristic, however, the bandwidth terms will generally be different. A comparison of these three definitions of bandwidth for the rectangular and Hanning data windows is seen below in table 2.1.

Data Window	B_r	B_n	B_s
Rectangular	$\frac{.85}{L}$	$\frac{1}{L}$	$\frac{1.23}{L}$
Hanning	$\frac{1.4}{L}$	$\frac{1.5}{L}$	$\frac{2.08}{L}$

Table 2.1. Comparison of Bandwidth Definitions

For finite records, the extent to which the width of peaks can be estimated and fine detain detected is also influenced by the variance of the estimate. Hence, to be able to trust the fine structure of the spectrum, it must be possible to tie down the estimate to a given stability. The estimator is said to have high stability if the variance of the smoothed spectral estimate is small. A convenient description of a spectral estimate is given by its "equivalent number of degrees of freedom", K, defined (Blackman and Tukey, 1968) as

$$K = \frac{2(\text{Average})^2}{\text{Variance}} \tag{2.49}$$

Since a small variance is associated with a stable estimate, the larger the equivalent number of degrees of freedom the more stable the estimate. It will be shown in section III that maximum stability is obtained by overlapping the data windows as shown in figure 2.17. The amount of overlap used to achieve the maximum stability is dependent upon the particular data window used. For a fixed transform length L, windows with lower sidelobes have wider and smoother main lobes and therefore require less overlap to achieve maximum stability.

In addition to the fidelity and stability of the estimated spectrum, there are some other important considerations to be made when choosing the parameters to be used in making the estimates. For instance, the

statistics of the background must be a factor in determining the length of time, T, used in the smooth estimates. A particular advantage to this method of obtaining the spectral estimates is that L may be chosen so that slow variations in the background do not affect the performance of the processor. If necessary, the frequency resolution of the estimate may be adjusted by appending zeros to the data before taking the transforms.

Additionally, if the desired signal is unstable - i.e., fading in and out due to the effects of the propagation medium, propagation paths, or just being transmitted intermittently - and therefore not present for at least lengths of time equal to T, then it is possible that the integration process will actually attenuate the signal rather than enhance it. Redundancy is the display will help alleviate the intermittent transmission problem by providing the operator with estimates which are not totally independent, but fade-in and fade-out problems due to propagation should be considered in choosing the integration time T.

III. THE SPECTRAL ESTIMATE

In the development of modern communication theory, a vast body of knowledge involving various technical disciplines has been incorporated. The area of digital data analysis and measurement, for example, includes the widespread use of spectral analysis techniques made feasible by the availability of the fast Fourier transform algorithm. Increased emphasis on optimization and detection techniques also necessitates the use of modern statistical procedures. The very foundation of communication engineering includes such topics as probability theory, random processes, and information theory. This section will draw on what is necessary from the theoretical framework of modern communication theory to discuss the problem of estimating the power spectra of finite length records and determining their confidence level.

A. STATIONARY STOCHASTIC PROCESSES AND ERGODICITY

A process is termed deterministic if it does not contain any features of randomness; otherwise it is termed stochastic (or random). Spectral analysis is concerned mainly with a class of stochastic processes called stationary stochastic processes. A stationary stochastic process is one whose statistical properties do not change with time. Signals generated by a stationary process have the property that a long enough segment of any signal recorded in some time period has essentially the same statistics as another segment of the signal observed at some other period. That is, a signal from a stationary process is not tied down to any particular origin in time.

There are several definitions of stationarity in current use. A

process is said to be stationary in the strict sense if none of the statistics which characterize the stochastic process changes with time. Another definition of stationarity is wide-sense or weak stationarity. A process is said to be weakly stationary if the mean value and auto-correlation function do not vary with time. In other words, for the weakly stationary random process, the mean value is a constant and the auto-correlation function is dependent only upon the displacement τ and not on the particular time chosen to compute the auto-correlation.

If each signal of the ensemble of possible signals that can be generated by a stationary process is typical of the ensemble as a whole, then the process is said to be ergodic. The statistics over a long time interval for any one signal are then the same as the statistics over the ensemble of all possible signals at any one time instant. Thus an ergodic process is one for which corresponding ensemble averages and time averages are equal.

The class of ergodic processes is a subclass of the class of stationary processes. That is, an ergodic process is necessarily stationary but a stationary process need not be ergodic. The application of theory to practice is very often simplified by making the assumption that a process is ergodic; however, except in special instances it would be difficult or impossible to demonstrate that a physical process is ergodic other than by direct measurements and comparisons.

B. DEFINITION

The following discussion will examine the definition of the spectral estimate, the error involved in trying to make a spectral estimate from a finite length sample, and ways of improving this inherent error. To avoid confusion, the terms "spectral estimate" or "estimate" in this discussion

refer consistently to the estimate of each individual spectral component within the bandwidth of interest, B; and the term "spectrum" will be used to refer to all the individual estimates collectively.

In order to proceed with estimating the spectrum of ocean ambient noise, some assumptions about the properties of the noise will have to be made. It will be assumed in this discussion that the ocean ambient noise may be considered approximately Gaussian and at least weakly stationary. Some recent research has shown that these assumptions are reasonable (Parkins, 1968).

In the context of digital signal processing, the power spectral density or power spectrum of a signal is defined as the magnitude squared of the Fourier transform of the signal. Inherent in the definition of the Fourier transform, however, is the fact that a signal of finite length will have a transform which contains all frequencies and, conversely, a band-limited spectrum emanates from a signal which extends from $t = -\infty$ to $t = +\infty$. Therefore, in order to talk about a finite spectrum, the definition of the true power spectrum of a record n(t) is defined as

$$G(f) = \lim_{T\to\infty} \frac{2}{T} E\left[|N(f,T)|^2 \right] \tag{3.1}$$

where N(f,T) is the finite Fourier transform of n(t), that is,

$$N(f,T) = \int_0^T n(t)\, e^{-j2\pi ft}\, dt \tag{3.2}$$

An estimate of the true spectrum given in Equation 3.1 for a sample record of any length T may be obtained by simply omitting the limiting and expectation operators. This will yield an estimated spectrum of

$$\hat{G}(f,T) = \frac{2}{T} |N(f,T)|^2 \tag{3.3}$$

where the frequency resolution will be $\frac{1}{T}$. This estimate, as it stands, will be shown to be statistically unreliable, however. Methods of improving the reliability will be presented in Section IIIE.

C. STATISTICS OF THE SPECTRAL ESTIMATE

As we discussed in Section II, N(f,T) is a complex quantity composed of the real and imaginary Fourier coefficients and $|N(f,T)|^2$ is the sum of the squares of the Fourier coefficients. Now, since n(t) is considered to be a Gaussian random process with zero mean, and since the Fourier transform is a linear operation, it can easily be shown (see Section IV) that the Fourier coefficients are independent Gaussian random variables with zero mean and equal variances.

Blackman and Tukey (Pg 21) show that each frequency estimate of $\hat{G}(f)$ is a chi-square variable with two "degrees of freedom". The number of degrees of freedom, K, may be thought of as representing the number of independent or "free" squares entering into the estimate. Note that Equation 3.3 describes the estimated spectrum and that each spectral component is a chi-square variable with two degrees of freedom. The probability density function of χ_k^2 is given by

$$P_{\chi_k^2}(x) = [2^{k/2}\,\Gamma(k/2)]^{-1}\, x^{(k/2-1)}\, e^{-x/2} \tag{3.4}$$

where

$$\Gamma(a) = \int x^{a-1}\, e^{-x}\, dx \tag{3.5}$$

The mean and variance of the variable χ_k^2 are

$$E[\chi_k^2] = \mu_{\chi_k^2} = k \tag{3.6}$$

$$\mathrm{Var}[\chi_k^2] = \sigma 2_{\chi_k^2} = 2k \tag{3.7}$$

Note that the variance of the spectral estimate is independent of the record length T. That is, increasing the record length does not reduce the variance of the estimate; it only increases the number of spectral components in the spectrum. Since the record length is a measure of the sample size for the estimate, this implies that the PSD estimates given by Equation 3.3 are inconsistent. To be consistent, an estimate should approach the parameter being estimated with a probability approaching unity as the sample size becomes large. That is, for any $\varepsilon > 0$,

$$\lim_{T\to\infty} \text{Prob}\left[\left|\hat{G} - G\right| \geq \varepsilon\right] = 0 \tag{3.8}$$

Because the estimates given by Equation 3.3 are inconsistent, the spectrum computed from that equation is called the "raw spectrum" and the components of the spectrum are called the "raw" components. It will be shown that more nearly consistent estimates can be made by "smoothing" the raw estimates.

D. ERROR ASSOCIATED WITH THE SPECTRAL ESTIMATE

The accuracy of parameter estimates based upon sample values is usually described in terms of the mean square error defined by

$$\text{Mean square error} = E\left[(\hat{G} - G)^2\right] \tag{3.9}$$

It can easily be shown that the mean square error is made up of two parts; the variance of the estimate (random error) and the square of the bias error of the estimate, that is,

$$\text{Mean square error} = \text{Var}\left[\hat{G}\right] + b^2[\hat{G}] \tag{3.10}$$

An estimate is said to be unbiased if $E[\hat{G}] = G$. Therefore, the bias error of the estimate is defined as

$$\text{Bias error} = b[\hat{G}] = E[\hat{G}] - G \tag{3.11}$$

In Bendot and Piersol (Pg 187), the bias error for the spectral estimate is shown to be proportional to the second derivative of the true spectrum. Therefore, for a relatively smooth spectrum over the effective bandwidth B_e of each estimate, the bias error is usually negligible compared with the random portion of the error, VAR[G]. The mean square error is thus approximately equal to the square of the standard error where the standard error is defined as

$$\text{Standard error} = \sqrt{\text{VAR}[\hat{G}]} = \sigma[\hat{G}] \tag{3.12}$$

If this error is expressed as a fraction of the quantity being estimated, it is called the normalized standard error, ε_r, and is given by

$$\varepsilon_r = \frac{\sigma[\hat{G}]}{G} \tag{3.13}$$

Remembering that

$$E[\chi_k^2] = E[\hat{G}] = k \simeq G \tag{3.14}$$

and

$$\text{VAR}[\chi_k^2] = \text{VAR}[\hat{G}] = 2k \tag{3.15}$$

we have

$$\varepsilon_r = \sqrt{\frac{2}{k}} \tag{3.16}$$

And since K = 2 for the raw spectral estimate, we have a standard error of unity, which says that the standard deviation of the estimate is as large as the quantity being estimated — which is obviously unacceptable. The smoothing operations presented in the next section will increase the number of degrees of freedom associated with each estimate and thus decrease the standard error considerably.

E. SMOOTHING THE SPECTRAL ESTIMATE

The method of reducing this error is called "smoothing" and may be

accomplished in one of two ways. The first way is to smooth over an ensemble of estimates. This can be done by computing individual estimates from q sample records and then averaging the q estimates at each frequency. The second way is to smooth over frequency. This can be done by averaging together the results of ℓ contiguous spectral components in the estimate from a single sample record. In either case, the smoothing operation approximates the expectation operation in equation 3.1 and hence makes the estimates consistent.

For ensemble smoothing, the estimates from q independent (i.e., non-overlapping) time slices are averaged together. If each time slice is of length T', then the length of the original sample is T = qT' and the final smoothed estimate is given by

$$\hat{G}_i = \frac{1}{q}\left[\tilde{G}_{i,1} + \tilde{G}_{i,2} + \ldots + \tilde{G}_{i,q}\right] \tag{3.17}$$

where $\tilde{G}_{i,q}$ is the raw estimate at frequency f_i of the q^{th} time slice. Noting that $\chi_a^2 + \chi_b^2 = \chi_{a+b}^2$ we see that the smoothed estimate will be a chi-squared variable with roughly 2q degrees of freedom. The smoothing operation did not affect the bandwidth of the estimates; hence each estimate will have an effective bandwidth of $B_e = \frac{\alpha}{T}$, where α depends on the particular window being used. Hence, by ensemble averaging

$$B_e = \frac{\alpha}{T'} = \frac{\alpha q}{T} \tag{3.18}$$

and

$$\varepsilon_r = \sqrt{\frac{2}{k}} = \sqrt{\frac{1}{q}} \tag{3.19}$$

The filter shape of each smooth estimate will be the same as for the raw estimate which is determined by the Fourier transform of the original data window used. The estimate $\hat{G}_i$ is considered as representing the

midpoint of the frequency interval covered by the filter (B_e is the effective bandwidth of the filter). Figure 3.1 illustrates the process of obtaining smooth spectral estimates using ensemble averaging.

For frequency smoothing, the estimates of ℓ contiguous spectral components from the raw spectrum are averaged to form the smooth estimate (the raw spectrum referred to was computed from a time record of length T). Hence, the i^{th} spectral component $\hat{G}_i$ of the smoothed spectrum will be given by

$$\hat{G}_i = \frac{1}{\ell}\left[G_{\frac{2i+1-\ell}{2}} + \ldots + G_{\frac{2i-1+\ell}{2}} \right] \tag{3.20}$$

where G_i is the i^{th} component of the raw estimate and it is assumed that ℓ is odd. $\hat{G}_i$ will be a chi-squared variable with roughly 2ℓ degrees of freedom by the same reasoning used with ensemble smoothing. The effective bandwidth, B'_e, of the smoothed estimate will depend on the value of ℓ and will be given by

$$B'_e = \frac{\ell - 1 + \alpha}{T} \tag{3.21}$$

where the effective bandwidth of each raw estimate used in the average was $B_e = \alpha/T$. Again the value of α depends on the data window used. The filter shape of the smoothed estimate will be approximately trapezoidal as shown in figure 3.2. The process of obtaining a smooth estimate through frequency averaging is shown in figure 3.3. The estimate $\hat{G}_i$ is considered as representing the midpoint of the frequency interval covered by B_e. A total of N/ℓ independent estimates can be obtained in the smoothed spectrum. The standard error of the estimates obtained by frequency averaging is given by

$$\varepsilon_r = \sqrt{\frac{2}{k}} = \sqrt{\frac{1}{\ell}}$$

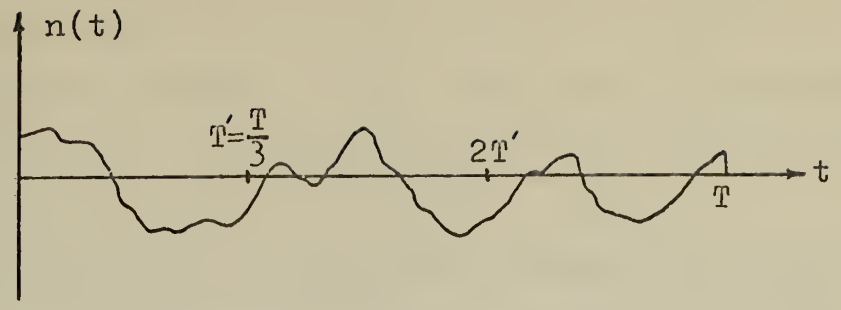

(a) Sample record segmented into three pieces

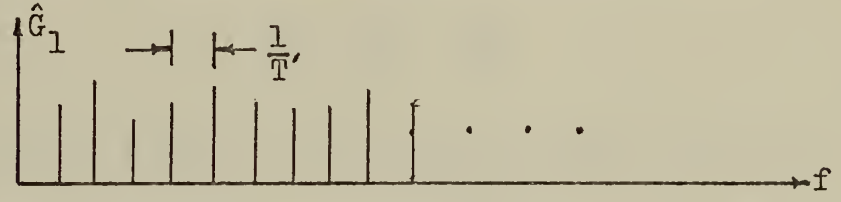

(b) Raw spectrum from segment one

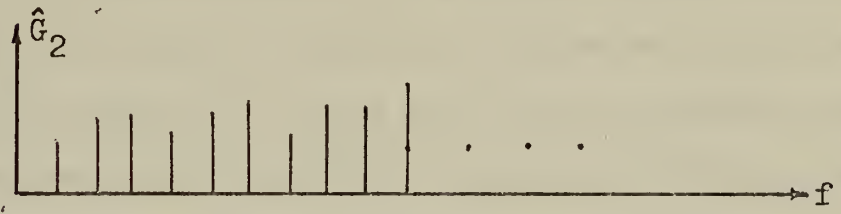

(c) Raw spectrum from segment two

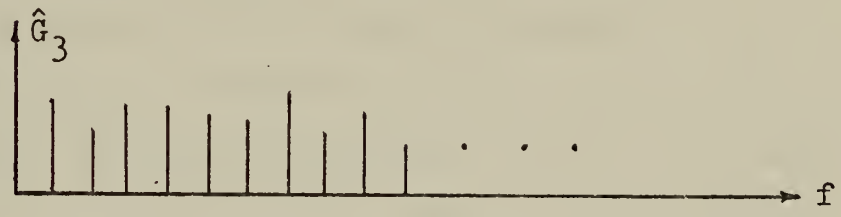

(d) Raw spectrum from segment three

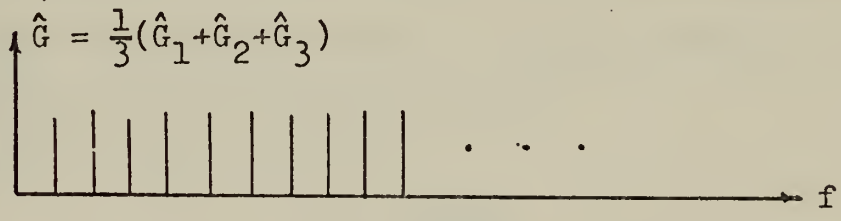

(e) Smoothed spectrum by ensemble smoothing with q=3

Figure 3.1. Example of ensemble smoothing

For combined smoothing using both frequency and ensemble averaging, the final effective bandwidth of each estimate will be approximately

$$B'_e = \frac{\ell}{T'}$$

and the resulting $\hat{G}_i$ will be a chi-squared variable with roughly $2\ell q$ degrees of freedom. The normalized standard error ε_r is given by

$$\varepsilon_r = \sqrt{\frac{2}{k}} = \sqrt{\frac{1}{\ell q}} \tag{3.24}$$

Even though the stability of the estimates may be improved by either ensemble or frequency smoothing or a combination of the two, it is advisable to use only ensemble smoothing in a system designed to detect narrow-band signals. The frequency resolution of the estimated spectrum will generally be determined to be of the same order of magnitude as the signal to be detected, and taking longer transforms and frequency smoothing would be a very inefficient use of the available resources.

F. INCREASED STABILITY THROUGH OVERLAPPING SEGMENTS

The term "degrees of freedom" introduced in Section IIIC as a measure of the stability of the estimate was said to refer to the number of independent or "free" squares that were summed to form the estimate. A slightly relaxed definition of the number of degrees of freedom of an estimate, called the "equivalent number of degrees of freedom", can be used by noting that for a chi-squared variable

$$K = \frac{2E^2[\hat{G}]}{Var[\hat{G}]} \tag{3.25}$$

This definition of K will be used to see if the stability of the estimates may be increased still further by overlapping the segments used in the ensemble smoothing operation.

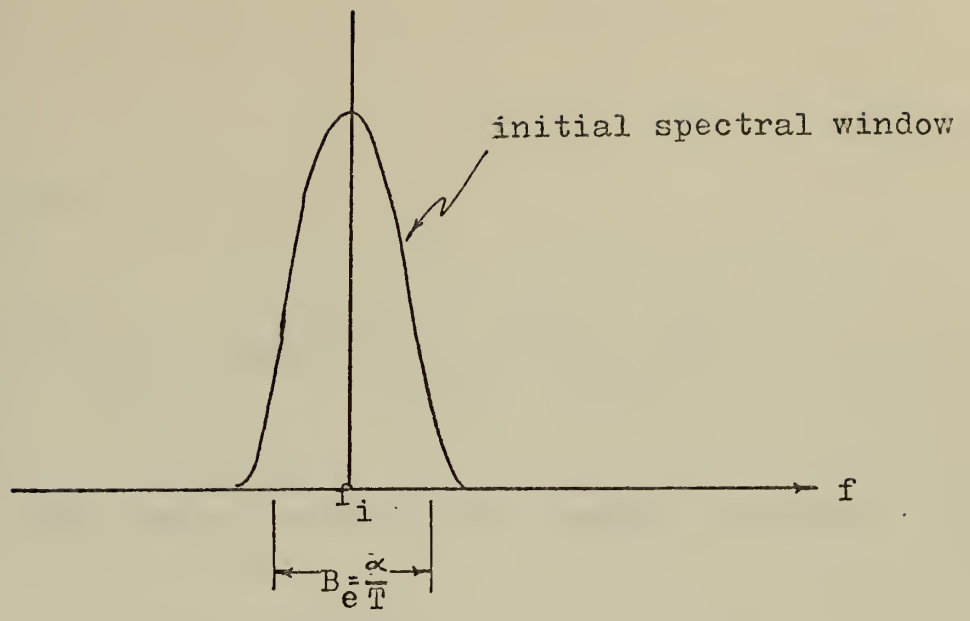

(a) Filter shape before frequency smoothing

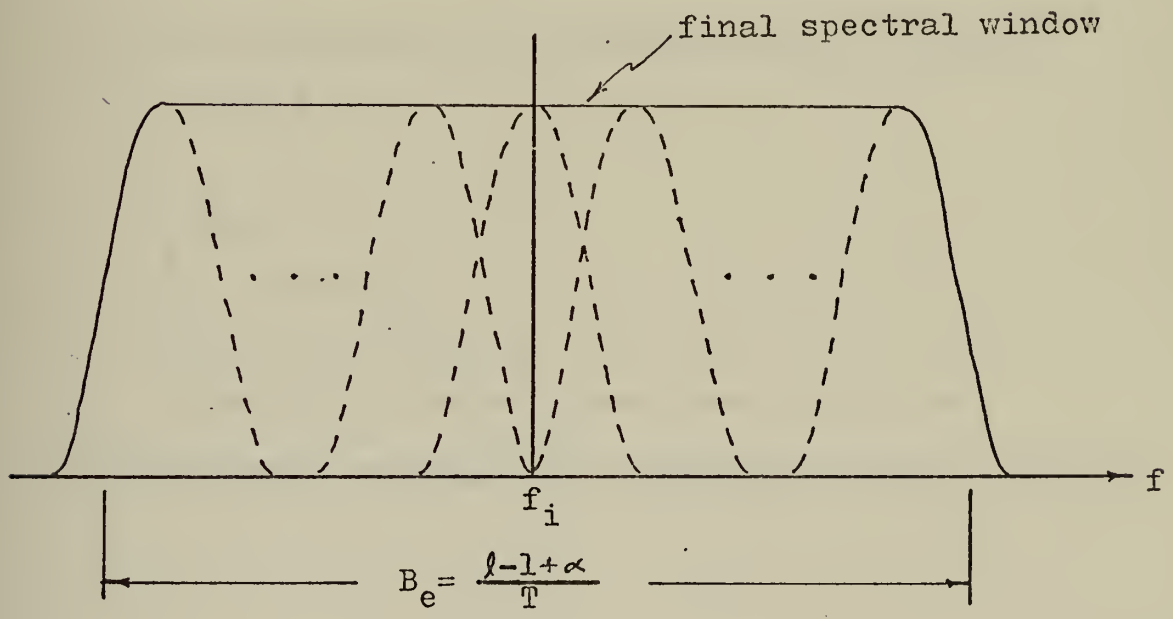

(b) Filter shape after frequency smoothing

Figure 3.2. Filter shape before and after freq.smoothing

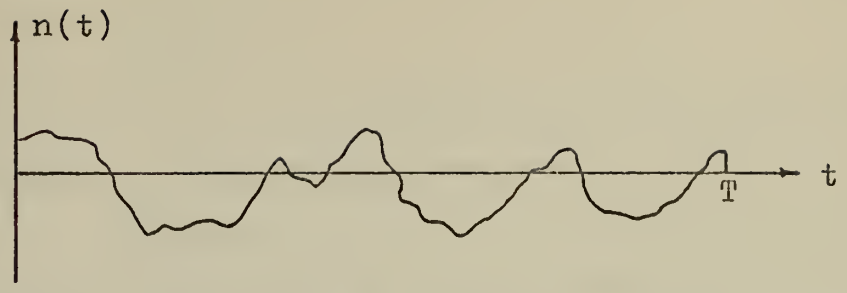

(a) Sample record used for the spectral analysis

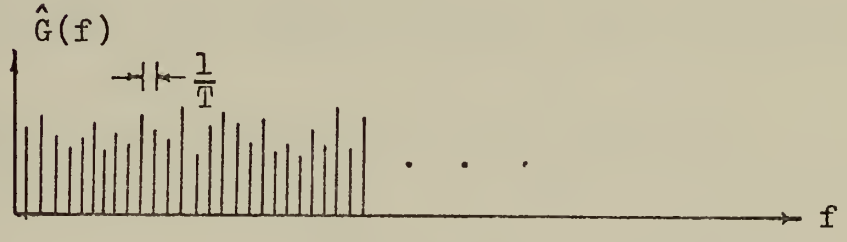

(b) Raw spectrum from transform of n(t) between t = 0 and t = T

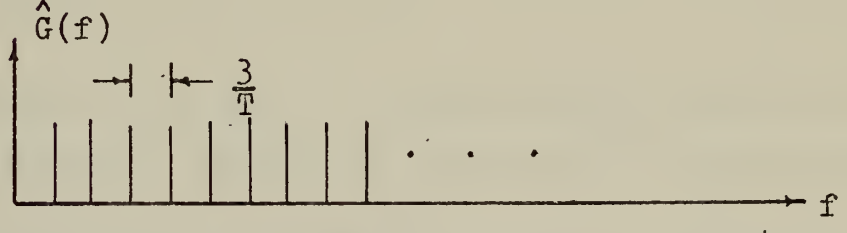

(c) Smoothed estimate by frequency smoothing with $\ell = 3$

Figure 3.3. Example of frequency smoothing

Referring to the notation of section 2.2.5 and figure 2.17, we see that each smooth estimate is computed by

$$\hat{G}(f) = \frac{1}{P} \sum_{i=1}^{P} \left|\tilde{G}_i(f)\right|^2 \tag{3.26}$$

where $G_i(f)$ is the finite Fourier Transform of the ith windowed section and P is the number of segments used. That is

$$\tilde{G}_i(f) = \int_{\frac{L}{2}+(i-1)s}^{\frac{3L}{2}+(i-1)s} n(t)\, W[t - \frac{L}{2} - (i-1)s]e^{-j2\pi ft}dt, \qquad 1 \leq i \leq P \tag{3.27}$$

The spectral estimate G(f) in equation 3.26 is a random variable. Its mean and variance were computed by Nuttall (1971) and are given by

$$E[\hat{G}(f)] = \int_{-\infty}^{\infty} G(f - \nu)\left|W(\nu)\right|^2 d\nu \simeq G(f) \int_{-\infty}^{\infty} \left|W(\nu)\right|^2 d\nu \tag{3.28}$$

$$Var[\hat{G}(f)] = G^2(f) \frac{1}{P} \sum_{i=-(P-1)}^{(P-1)} (1 - \frac{|i|}{P})\left|\phi_w(is)\right|^2 \tag{3.29}$$

where

$$\phi_w(\tau) = \int_{-\infty}^{\infty} W(t)\, W(t - \tau)dt \tag{3.30}$$

under the assumption that n(t) is a Gaussian random process and that the frequency resolution of the spectral window $\left|W(f)\right|^2$ is narrower than the finest detail in the true spectrum G(f).

Equation 3.28 shows that the mean of the spectral estimate is equal to the convolution of the true spectrum G(f) with the spectral window $\left|W(f)\right|^2$. Equation 3.29 expresses the variance of the spectral estimate in terms of the number of pieces P, the shift S, and the autocorrelation ϕ_w of the data window. Using the results given in equations 3.28 and 3.29, we can compute the equivalent number of degrees of freedom of our

estimate in terms of the number of pieces used and the autocorrelation of the data window as follows:

$$K = \frac{2E^2[\hat{G}(f)]}{Var[\hat{G}(f)]} \tag{3.31}$$

$$= \frac{2P\left[\int |W(\nu)|^2 d\nu\right]^2}{\sum_{i=-(P-1)}^{P-1} (1 - \frac{|i|}{P}) |\phi_w(iS)|^2} \tag{3.32}$$

But $$\phi_w(0) = \int_{-\infty}^{\infty} W^2(t)dt \tag{3.33}$$

$$K = \frac{2P}{\sum_{i=-(P-1)}^{P-1} (1 - \frac{|i|}{P}) \left|\frac{\phi_w(iS)}{\phi_w(0)}\right|^2} \tag{3.34}$$

Notice that K is independent of the value of frequency f and true spectrum G(f). It depends only on the particular data window W and the number of pieces P. Noting that the shift S is uniquely determined as a function of P,L, and T, as shown in equation 2.44, we have

$$K = \frac{2P}{1 + 2\sum_{i=1}^{P-1} (1 - \frac{i}{P}) \left|\frac{\phi_w(i - \frac{T-L}{P-1})}{\phi_w(0)}\right|^2} \tag{3.35}$$

It is interesting to note that for a given T/L, a maximum value of K occurs at some value of overlap less than 100 percent. The value of overlap is a function of the particular data window used and is relatively independent of the value of T/L. As described in section IIC, for P = T/L, K = 2P. As P increases for a given T/L, the value of K will increase but at a continually decreasing rate because the overlapped pieces are progressively more statistically dependent. K will eventually

reach a maximum value and then decrease slightly as the amount of overlap approaches 100 percent. A typical curve of K versus percent overlap is shown in figure 3.4. Note that the amount of overlap required to achieve 90 or 95 percent of maximum stability is considerably less than that required for 100 percent. The extra computational effort required for highly overlapped processing should be given serious consideration before implementing the maximum value of K.

The rectangular data window is described by

$$W(t) = u(t) - u(t-L)$$

where u(t) is a step function.

The autocorrelation function as defined in equation 3.30 is computed to be

$$\phi(\tau) = L - |\tau| \qquad (|\tau| \leq L) \tag{3.36}$$

and

$$\frac{\phi(\tau)}{\phi(0)} = 1 - \frac{|\tau|}{L} \qquad (|\tau| \leq L) \tag{3.37}$$

For the Hanning window

$$W(t) = \frac{1}{2}\left(1 - \cos\frac{2\pi t}{L}\right)[u(t) - u(t - L)] \tag{3.38}$$

thus

$$\phi(\tau) = \frac{1}{4}(L-\tau)\left(1+\frac{1}{2}\cos\frac{2\pi\tau}{L}\right) + \frac{3}{16}\frac{L}{\pi}\sin\frac{2\pi\tau}{L} \qquad (|\tau| \leq L) \tag{3.39}$$

and

$$\frac{\phi(\tau)}{\phi(0)} = \frac{2}{3L}(L-\tau)\left(1+\frac{1}{2}\cos\frac{2\pi\tau}{L}\right) + \frac{1}{2\pi}\sin\frac{2\pi\tau}{L} \qquad (|\tau| \leq L) \tag{3.40}$$

Tables 3.1 - 3.4 show how K varies as a function of P for several values of T/L, as given by equation 3.35, for the rectangular and Hanning windows.

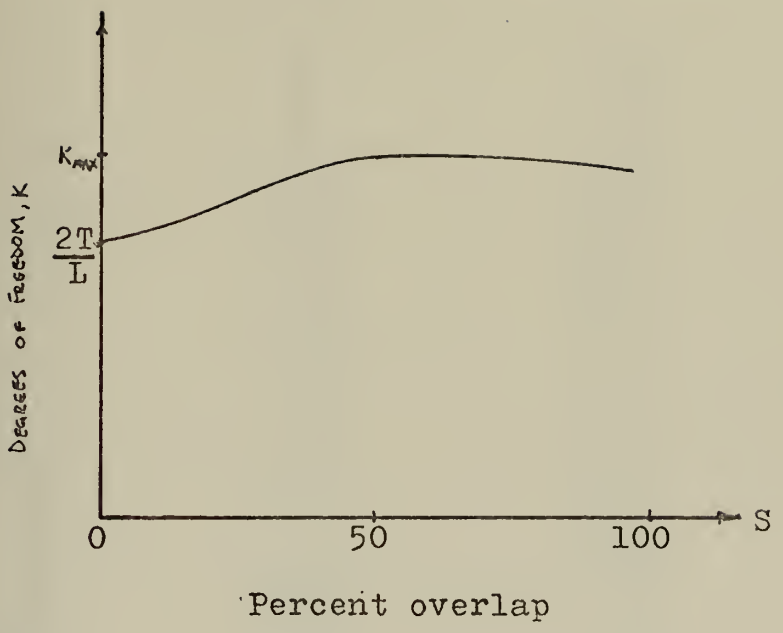

Figure 3.4. Typical K vs S curve

		RECTANGULAR	HANNING
P	S(%)	K	K
4	0	8.0	8.0
5	25	9.09	9.99
6	40	9.47	11.91
7	50	9.80	13.36
8	57.1	9.99	14.09
9	62.5	10.05	14.29
10	66.7	10.11	14.28
11	70.0	10.15	14.20
12	72.7	10.15	14.13
13	75.0	10.16	14.06
14	76.9	10.17	14.00
15	78.6	10.16	13.94
16	80.0	10.15	13.90
17	81.2	10.15	13.85
18	82.4	10.14	13.81
19	83.3	10.14	13.78
20	84.2	10.13	13.75
50	93.9	9.98	13.38
100	97.0	9.90	13.26
200	98.5	9.86	13.20
300	99.0	9.85	13.18
400	99.2	9.84	13.17
500	99.4	9.83	13.16

TABLE 3.1 K vs P FOR T/L = 4

		RECTANGULAR	HANNING
P	S(%)	K	K
8	0	16.0	16.0
9	12.5	17.51	18.0
10	22.2	18.37	20.0
11	30.0	18.91	21.99
12	36.4	19.32	23.92
13	41.7	19.69	25.71
14	46.2	20.06	27.27
15	50.0	20.46	28.52
16	53.3	20.76	29.45
17	56.2	20.95	30.09
18	58.8	21.06	30.49
19	61.1	21.16	30.72
20	63.2	21.25	30.83
21	65.0	21.35	30.87
22	66.7	21.46	30.87
23	68.2	21.55	30.85
24	69.6	21.61	30.82
25	70.8	21.64	30.79
50	85.7	21.95	30.30
100	92.9	21.93	30.03
200	96.5	21.87	29.89
300	97.7	21.84	29.84
400	98.2	21.83	29.81
500	98.6	21.82	29.80

TABLE 3.2 K vs P FOR T/L = 8

		RECTANGULAR	HANNING
P	S(%)	K	K
16	0	32.0	32.0
17	6.2	33.75	34.0
18	11.8	35.08	36.0
19	16.7	36.10	38.0
20	21.1	36.89	40.0
25	37.5	39.37	49.77
30	48.3	41.36	57.67
35	55.9	42.87	62.07
40	61.5	43.49	63.70
45	65.9	44.05	64.06
46	66.7	44.19	64.070
47	67.4	44.31	64.074
48	68.1	44.40	64.073
49	68.7	44.48	64.067
50	69.4	44.55	64.06
100	84.8	45.66	63.59
200	92.5	45.85	63.30
300	95.0	45.85	63.20
400	96.2	45.84	63.15
500	97.0	45.83	63.12

TABLE 3.3 K vs P FOR T/L = 16

		RECTANGULAR	HANNING
P	S(%)	K	K
32	0	64.0	64.0
33	3.1	65.88	66.0
34	6.1	67.52	68.0
35	8.8	68.96	70.0
36	11.4	70.22	72.0
37	13.9	71.32	74.0
38	16.2	72.30	76.0
39	18.4	73.16	78.0
40	20.5	73.93	80.0
50	36.7	79.08	99.61
60	47.5	83.16	115.85
70	55.1	86.53	125.43
80	60.8	87.94	129.31
90	65.2	89.11	130.36
100	68.7	90.29	130.52
101	69.0	90.37	130.53
102	69.3	90.43	130.53
103	69.6	90.49	130.52
104	69.9	90.55	130.52
105	70.2	90.61	130.52
110	71.6	90.84	130.50
120	74.2	91.29	130.45
130	76.0	91.82	130.40
140	77.7	92.08	130.35
150	79.2	92.29	130.30
200	84.4	93.07	130.11
300	89.6	93.55	129.92
400	92.2	93.70	129.82
500	93.8	93.75	129.76

TABLE 3.4 K vs P FOR T/L = 32

G. CONFIDENCE INTERVAL FOR THE SPECTRAL ESTIMATE

Since the sampling distribution of the smoothed estimate is approximately chi-square with K degrees of freedom, we have a $(1 - \alpha)$ confidence interval for a power spectral density function G(f) (based upon an estimate $\hat{G}(f)$ measured with a resolution bandwidth B_e and a record length T) given by

$$\left[\frac{K\hat{G}(f)}{\chi^2_{K:\ \alpha/2}} \leq G(f) < \frac{K\hat{G}(f)}{\chi^2_{K:\ 1 - \alpha/2}} \right] \tag{3.41}$$

The confidence statement is interpreted as follows: The true PSD G(f) will fall within the noted interval with a confidence coefficient of $(1 - \alpha)$, or in more common terminology, with a confidence of $100(1 - \alpha)$ percent.

IV. PROCESSING GAIN OF A FOURIER PROCESSOR WITH INTEGRATION

A. INTRODUCTION

Section III discussed the spectral estimate by the use of the fast Fourier transform technique and the method of improving the estimates for a given record of finite length. It was shown that the measure of quality or reliability of the estimate is the mean square error (or variance) and that this error can be made arbitrarily small if a longer record were available. This situation often creates a three-way compromise among effort, resolution and stability (precision) of the estimate.

This section will interpret the stability of the spectral estimates in terms of processing gain within the context of a Fourier signal processor. Figure 4.1 shows a model of the system. Its mission is to detect the presence in a random noise background of discrete narrowband signals with random phase variation. The decision element of the syetem is assumed to be a human operator monitoring a display similar to the one discussed in section II c. The sensitivity of the processor is usually defined in terms of a minimum detectable signal for a given probability of detection and false alarm. Because of the presence of the human operator in the system, the level of minimum detectable signal is difficult to determine and will not be discussed. A brief look at the theory of signal detection by a human operator will be coverd in section V. It should be noted that the "processing gain" discussed in this section is derived under rather idealized conditions. The effects of redundency and Hanning weighting are considered but losses due to hardware limitations are not discussed. Losses due to actual implementation

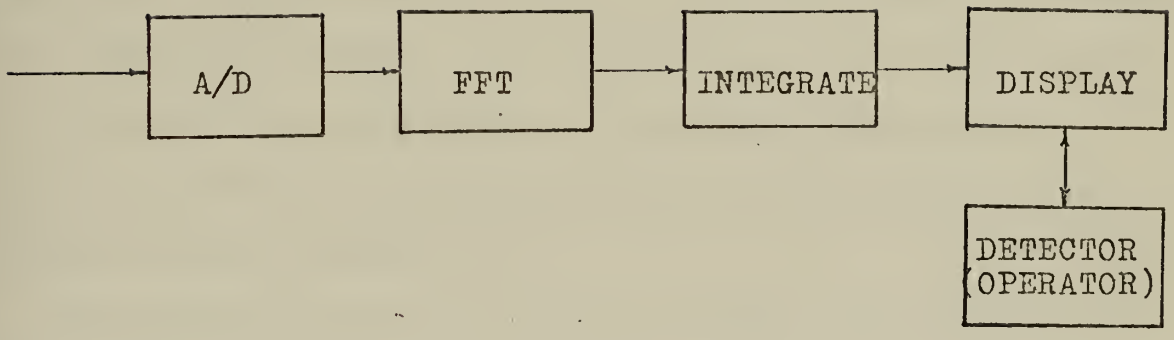

Figure 4.1. Fourier processor with integration

have been found to be small if careful consideration is given to the areas discussed in section II.

B. PROCESSING GAIN DEFINED

When talking about processing gain of a Fourier signal processor, it is convenient to view the DFT as a bank of N independent narrow band filters, where N is the number of equally spaced samples (each of width Δ) within the time of L the data to be transformed. The center of each "filter" will be located at multiples of the fundamental frequency $f_o = \frac{1}{L}$ Hz and the shape of each filter will depend upon the data window used as previously discussed. Regardless of which window is used, however, maximum power transfer will occur only if the desired signal if a multiple of the fundamental frequency. If the signal is not an even multiple of f_o, then it will be attenuated and its energy spread throughout the spectrum (the extent of the leakage will again depend on which window is used) as shown in figure 2.12.

The processing gain (PG) of a digital processor which utilizes the DFT as the initial filtering device and then incoherently integrates the output of each filter (i.e., ensemble smoothing) will be made up of two distinct parts, one part due to the DFT itself (PG_T) and one part due to the incoherent integration (PG_I). Heuristically, this makes sense, since the signal-to-noise power ratio (SNR) will obviously be improved by passing the signal through a narrowband filter. And then the results can be improved even more by averaging the random noise power over time since the average signal power is approximately constant. Therefore, the processing gain for the system is defined as

$$PG = PG_T \cdot PG_I \tag{4.1}$$

For simplicity, the processing gain will be derived in terms of a single discrete frequency component in an additive white gaussian noise background. The assumption of a white noise background is really not very restrictive since all that is required is that the power spectrum of the noise be flat over the bandwidth of each filter. Further, it will be assumed that the signal to be "detected" will be an integer multiple of the fundamental frequency, $f_o = 1/L$, so that maximum power transfer is achieved by the filter. This is a reasonable assumption since we are interested in the maximum gain available from the system. Also, it will be assumed that the signal is stable in frequency throughout the interval of observation and that it is actually present in the background during that time. Exceptions to the above assumptions will be discussed later.

The processing gain of each section of the processor will be defined as the ratio of the signal-to-noise power at the output of the section to the signal-to-noise power at the input of the section. For standardization, the noise power used is usually the average power of the noise in a 1 Hz band. Thus for the j^{th} filter of the DFT (see figure 4.2),

$$PG_{T,j} = \frac{SNR_2}{SNR_1} \tag{4.2}$$

and for the integrator

$$PG_{I,j} = \frac{SNR_4}{SNR_3} \tag{4.3}$$

Notice that the signal-to noise ratio at the output of the j^{th} filter is the input signal-to-noise ratio to the integrator (i.e., $SNR_2 = SNR_3$). Therefore,

$$PG_{T,j} \cdot PG_{I,j} = \frac{SNR_2}{SNR_1} \cdot \frac{SNR_4}{SNR_3} = \frac{SNR_4}{SNR_1} = PG_j \tag{4.4}$$

the processing gain for the entire system.

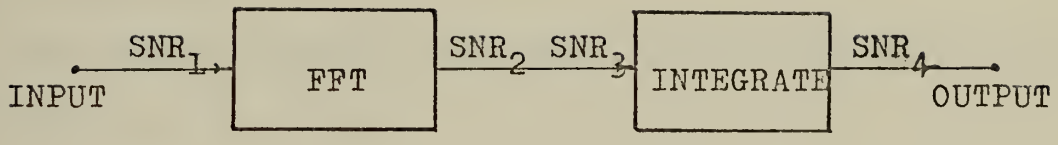

Figure 4.2. Reference for signal-to-noise ratios

For purposes of the following analysis, only the processing gain of a typical filter will be derived. Results for the remaining N-1 filters of the processor may be generalized from this one by considering whether or not a signal is present within the bandwidth of the filter.

C. PROCESSING GAIN OF THE DFT ($PG_{T,j}$)

The j^{th} filter output of the DFT is defined as

$$c_j = \frac{1}{N} \sum_{k=0}^{N-1} s_k e^{-i2\pi jk/N} \tag{4.5}$$

where s_k, k = 0,1,2,...,N-1 are the N sample values of the input signal to be transformed.

With noise only present at the input, the output of the j^{th} filter may be written as

$$c_j = \frac{1}{N} \sum_{k=0}^{N-1} n_k e^{-i2\pi jk/N} \tag{4.6}$$

where n_k, k = 0,1,2,...,N-1 are sample values from a zero mean Gaussian random process. In terms of the real and imaginary coefficients, the complex quantity c_j can be written as

$$c_j = a_j + i\, b_j \tag{4.7}$$

where

$$a_j = \mathrm{Re}(c_j) = \frac{1}{N} \sum_{k=0}^{N-1} n_k \cos(2\pi jk/N) \tag{4.8a}$$

$$b_j = \mathrm{Im}(c_j) = \frac{-1}{N} \sum_{k=0}^{N-1} n_k \sin(2\pi jk/N) \tag{4.8b}$$

Now since the DFT is a linear operator, the random variables a_j and b_j are each zero-mean Gaussian random variables when the input signal is noise alone. To show that a_j and b_j are also independent, we need only to show that $E[a_j b_j] = 0$.

Now

$$E[a_j b_j] = E[(\frac{1}{N}\sum_{k=0}^{N-1} n_k \cos 2\pi jk/N)(-\frac{1}{N}\sum_{\ell=0}^{N-1} n_\ell \sin 2\pi j\ell/N)] \quad (4.9)$$

$$= -\frac{1}{N^2}\sum_{k=0}^{N-1}\sum_{\ell=0}^{N-1} E[n_k n_\ell] \cos(2\pi jk/N) \sin(2\pi j\ell/N) \quad (4.10)$$

$$= -\frac{1}{N^2}\sum_{k=0}^{N-1} E[n_k^2] \cos(2\pi jk/N) \sin(2\pi jk/N) \quad (4.11)$$

$$= -\frac{\sigma^2}{N^2}\sum_{k=0}^{N-1} \sin(4\pi jk/N) \quad (4.12)$$

$$E[a_j b_j] = 0 \quad (4.13)$$

where σ^2 is the variance (average power) of the input noise signal.

Therefore, a_j and b_j are independent zero-mean Gaussian random variables. They also have equal variances as shown below:

$$Var[a_j] = E[a_j^2] = E[(\frac{1}{N}\sum_{k=0}^{N-1} k \cos 2\pi jk/N)(\frac{1}{N}\sum_{\ell=0}^{N-1} n_\ell \cos 2\pi j\ell/N)] \quad (4.14)$$

$$= E[\frac{1}{N^2}\sum_{k=0}^{N-1}\sum_{\ell=0}^{N-1} n_k n_\ell \cos(2\pi jk/N) \cos(2\pi j\ell/N)] \quad (4.15)$$

$$= \frac{1}{N^2}\sum_{k=0}^{N-1} E[n_k^2] \cos^2(2\pi jk/N) \quad (4.16)$$

$$= \frac{\sigma^2}{2N^2}\sum_{k=0}^{N-1} 1 + \cos(4\pi jk/N) \quad (4.17)$$

$$= \frac{\sigma^2}{2N} \quad (4.18)$$

And

$$Var[b_j] = E[b_j^2] = E[(\frac{1}{N}\sum_{k=0}^{N-1} n_k \sin 2\pi jk/N)(\frac{1}{N}\sum_{\ell=0}^{N-1} n_\ell \sin 2\pi j\ell/N)] \quad (4.19)$$

$$= \frac{1}{N^2} \sum_{k=0}^{N-1} E[n_k^2] \sin^2(2\pi jk/N) \tag{4.20}$$

$$= \frac{\sigma^2}{2N^2} \sum_{k=0}^{N-1} 1 - \cos(2\pi jk/N) \tag{4.21}$$

$$= \frac{\sigma^2}{2N} \tag{4.22}$$

Now the power spectral component of the j^{th} filter is defined as

$$\hat{G}_j = a_j^2 + b_j^2 \tag{4.23}$$

and the average power in that bin is therefore given by

$$\text{Avg Pwr} = E[\hat{G}_j] = E[a_j^2] + E[b_j^2] \tag{4.24}$$

$$= \frac{\sigma^2}{N} \tag{4.25}$$

Now if a signal is present, the sample values s_k, $k = 0,1,2,\ldots,N-1$ are each the sum of a zero mean Gaussian random variable and a constant $A \cos(2\pi fk\Delta + \phi)$. So the j^{th} filter output can be written as

$$C_j = \frac{1}{N} \sum_{k=0}^{N-1} [n_k + A \cos(2\pi fk\Delta + \phi)]e^{-i2\pi jk/N} \tag{4.26}$$

$$C_j = \frac{1}{N} \sum_{k=0}^{N-1} n_k e^{-i2\pi jk/N} + \frac{1}{N} \sum_{k=0}^{N-1} A \cos(2\pi fk\Delta + \phi)e^{-i2\pi jk/N} \tag{4.27}$$

which can be seen to be the sum of two independent parts, one due only to the noise and one due only to the signal. The noise portion was handled above. Consider now only the portion of the output due to the signal. Then,

$$C_{j,s} = \frac{A}{N} \sum_{k=0}^{N-1} \cos(2\pi fk\Delta + \phi)e^{-i2\pi jk/N} \tag{4.28}$$

$$= \frac{A}{2N} \sum_{k=0}^{N-1} [e^{i(2\pi fk\Delta + \phi)} + e^{-i(2\pi fk\Delta + \phi)}]e^{-i2\pi jk/N} \tag{4.29}$$

Now under the assumption that the signal is in the center of the bin we have $f\Delta = j/N$. So

$$C_{j,s} = \frac{A}{2N} \sum_{k=0}^{N-1} e^{i\phi} + e^{-i(4\pi jk/N + \phi)} \tag{4.30}$$

$$= \frac{A}{2} e^{i\phi}$$

The total output of the j^{th} bin with signal plus noise at the input is thus given by

$$C_j = \frac{A}{2} e^{i\phi} + \frac{1}{N} \sum_{k=0}^{N-1} n_k \, e^{-i2\pi jk/N} \tag{4.32}$$

$$= \left(\frac{A}{2} \cos \phi + \frac{1}{N} \sum_{k=0}^{N-1} n_k \cos 2\pi jk/N\right) - i\left(\frac{A}{2} \sin \phi + \frac{1}{N} \sum_{k=0}^{N-1} n_k \sin 2\pi jk/N\right) \tag{4.33}$$

The power spectral component at frequency j/N is given by

$$\hat{G}_j = |C_j|^2 \tag{4.34}$$

$$\hat{G}_j = \frac{A^2}{4} + \frac{A}{N} \cos \phi \sum_{k=0}^{N-1} n_k (2\pi jk/N) + \frac{A}{N} \sin \phi \sum_{k=0}^{N-1} n_k \sin(2\pi jk/N) + \frac{1}{N^2} \sum_{k=0}^{N-1} n_k^2 \tag{4.35}$$

and the average power at that frequency is given by

$$\text{Avg Pwr} = E[\hat{G}_j] \tag{4.36}$$

$$= \frac{A^2}{4} + \frac{\sigma^2}{N} \tag{4.37}$$

since $E[N_k] = 0$. Notice that the average power in the j^{th} bin is made up of two components, one due only to the noise and one due only to the signal. This is not an unexpected result since the noise and the signal were uncorrelated and therefore, the power should be additive.

Referring to equation 4.2, we are now ready to compute $PG_{T,j}$. The signal-to-noise ratio of the input signal is given by

$$SNR_1 = \frac{A^2}{2\sigma^2} \tag{4.38}$$

where σ^2 is the average power (variance) of the noise and $A^2/2$ is the RMS signal power. From 4.37 it is obvious that

$$SNR_2 = \frac{A^2 N}{4\sigma^2} = \frac{N}{2} SNR_1 \tag{4.39}$$

$$\text{therefore} \quad PG_{T,j} = \frac{SNR_2}{SNR_1} = \frac{N}{2} \tag{4.40}$$

which is a realistic result since the original noise power has been effectively separated into N/2 bins (see symmetry conditions of the DFT in section IIB) and the average siganl power is totally contained within the j^{th} bin.

D. PROCESSING GAIN OF THE INTEGRATOR AND TOTAL SYSTEM GAIN

The processing gain due to incoherent integration in the j^{th} bin is due entirely to the variance reduction (or smoothing) of the noise. This may be seen as follows:

$$SNR_3 = SNR_2 = \frac{A^2/4}{\sigma_3^2/N} \tag{4.41}$$

$$\text{and} \quad SNR_4 = \frac{A^2/4}{\sigma_4^2/N} \tag{4.42}$$

where σ_3^2 and σ_4^2 are the variances in the j^{th} bin due to the noise at stages three and four, respectively, of figure 4.2. Referring to Equation 4.3 we see that

$$PG_{I,j} = \frac{SNR_4}{SNR_3} = \frac{\sigma_3^2}{\sigma_4^2} \tag{4.43}$$

The variance of the smoothed spectral estimate was computed by Nuttall (1971) and is given by

$$\mathrm{Var}[\hat{G}] = \frac{G^2(f)}{P} \sum_{i=-(P-1)}^{(P-1)} \left(1 - \frac{|i|}{P}\right) \left|\phi_w(iS)\right|^2 \tag{4.44}$$

$$= \frac{G^2(f)}{P} \left\langle \left|\phi_w(0)\right|^2 + 2 \sum_{i=1}^{P-1} \left(1 - \frac{i}{P}\right) \left|\phi_w(iS)\right|^2 \right\rangle \tag{4.45}$$

where $G(f)$ = true spectrum of noise

$\phi_w(\tau)$ = autocorrelation function of the data window

P = number of raw transforms averaged to obtain the estimate

S = amount of overlap used in the P transforms in seconds.

The reader is referred to figure 2.17 and section III F for a review of how the above parameters relate.

Now, for the raw spectral estimate (i.e., estimate available at stage 3 of figure 4.2) P = 1 and we have no overlap. Therefore

$$\sigma_3^2 = G^2(f) \left|\phi_w(0)\right|^2 \tag{4.46}$$

For the smooth spectral estimate (i.e., estimate at the output of the integrator), P>>>1 and we have

$$\sigma_4^2 = \frac{G^2(f)}{P} \left\langle \left|\phi(0)\right|^2 + 2 \sum_{i=1}^{P-1} \left(1 - \frac{i}{P}\right) \left|\phi_w(iS)\right|^2 \right\rangle \tag{4.47}$$

Therefore

$$PG_{I,j} = \frac{P}{1 + 2 \sum_{i=1}^{P} \left(1 - \frac{i}{P}\right) \left|\frac{\phi_w(iS)}{\phi_w(0)}\right|^2} \tag{4.48}$$

$$= \frac{K}{2} \tag{4.49}$$

where K is the equivalent number of degrees of freedom of the estimate (see section 3). Note that if P = T/L, there is no overlap and $PG_{I,j} = P$. For P > T/L, the processing gain will be greater than P. Combining equation 4.49 and equation 4.40, the system processing gain is given by

$$PG = \frac{NK}{4} \tag{4.50}$$

To maximize the system processing gain for a given T/L, we want to overlap the transforms so as to maximize the value of K. Figure 4.3 shows that K_{max} is linear as a function of T/L if the Hanning window is used on the data. Similar results could be obtained for any data window using equation 3.35. Figure 4.4 shows the amount of overlap required to obtain K_{max}, $.99K_{max}$ and $.95K_{max}$ as a function of T/L. Note that while the amount of overlap required to obtain K_{max} increases slightly with T/L, the overlap required to obtain $.99K_{max}$ or $.95K_{max}$ is nearly independent of T/L. The slight discontinuities in figure 4.4 at small values of T/L are due to the large percentage overlap changes with the addition of one piece (or transform). Thus, for the Hanning window it would seem that 60 % overlap would be the optimum overlap from a processing gain point of view. Figure 4.5 shows how the value of K varies as a function of T/L if other than optimum overlap is used.

From figure 4.3 we see that

$$K_{max} = 4.15 \left(\frac{T}{L}\right) - 2.20 \tag{4.51}$$

So

$$PG = N(1.0375\ T/L - .55) \tag{4.52}$$

or in decibels,

$$PG = 10 \log_{10} N + 10 \log_{10}(1.0375\ T/L - .55)\ \text{db} \tag{4.53}$$

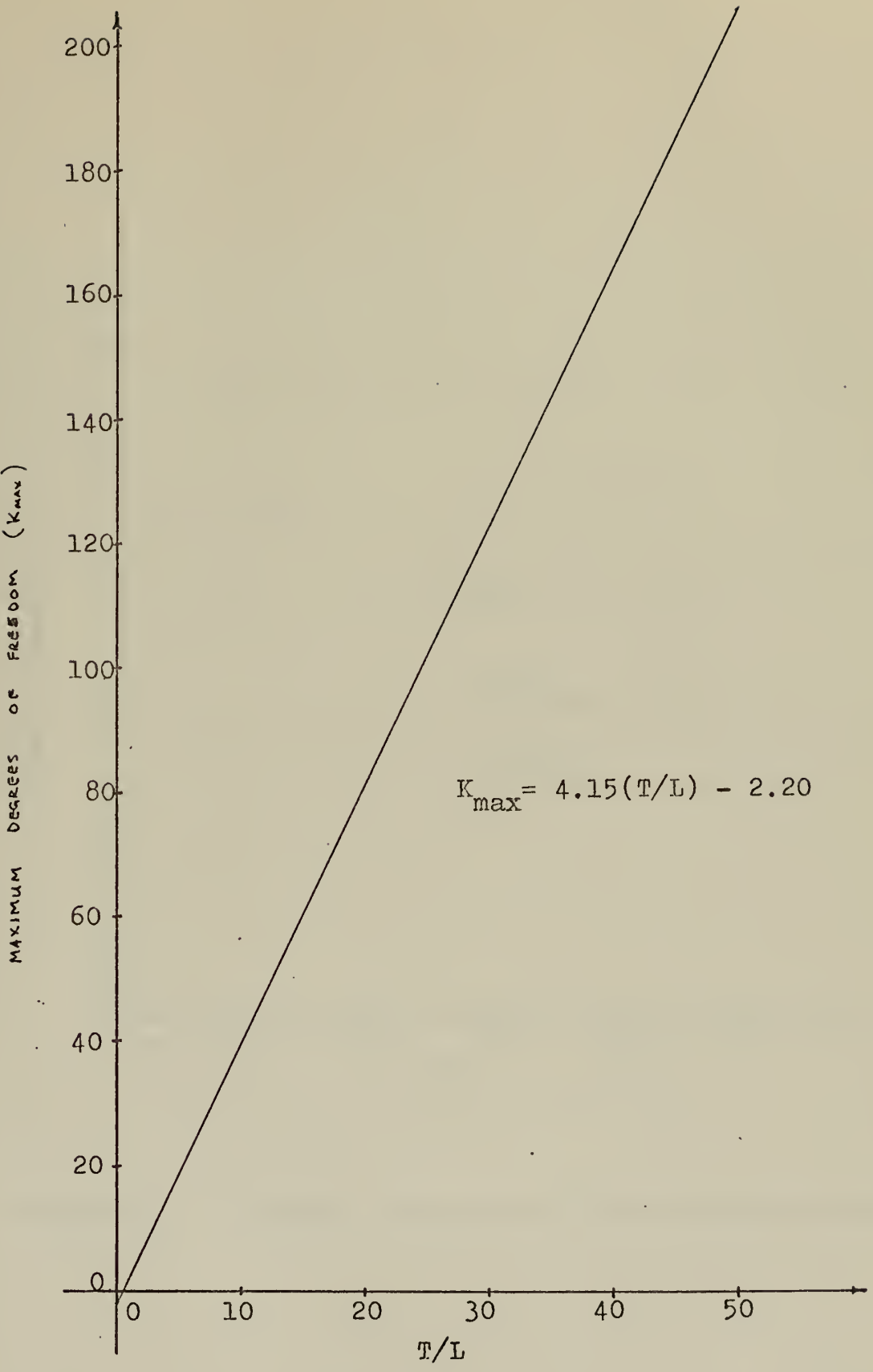

Figure 4.3. K_{max} vs T/L for Hanning window

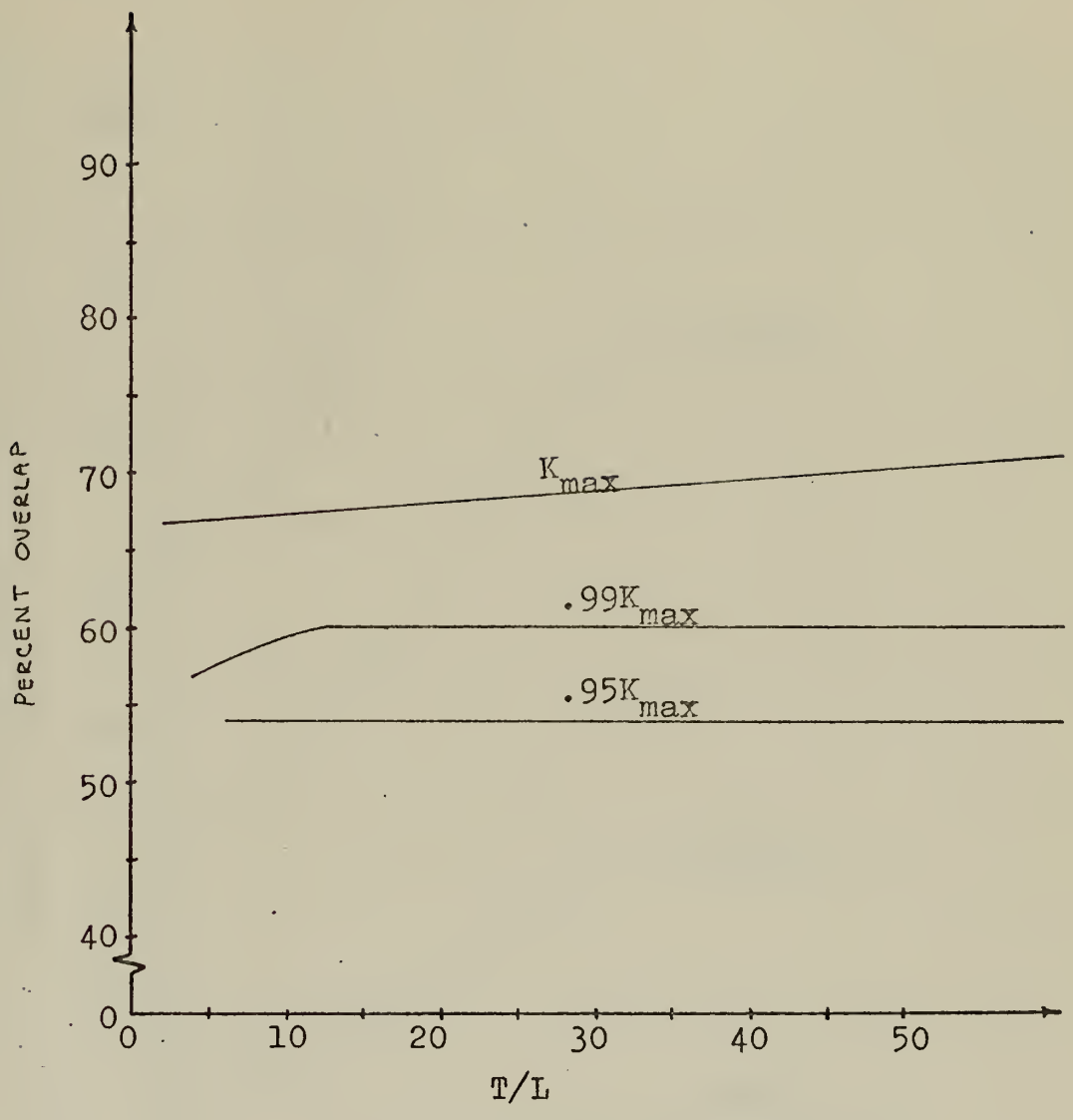

Figure 4.4. Percent overlap vs T/L for Hanning window

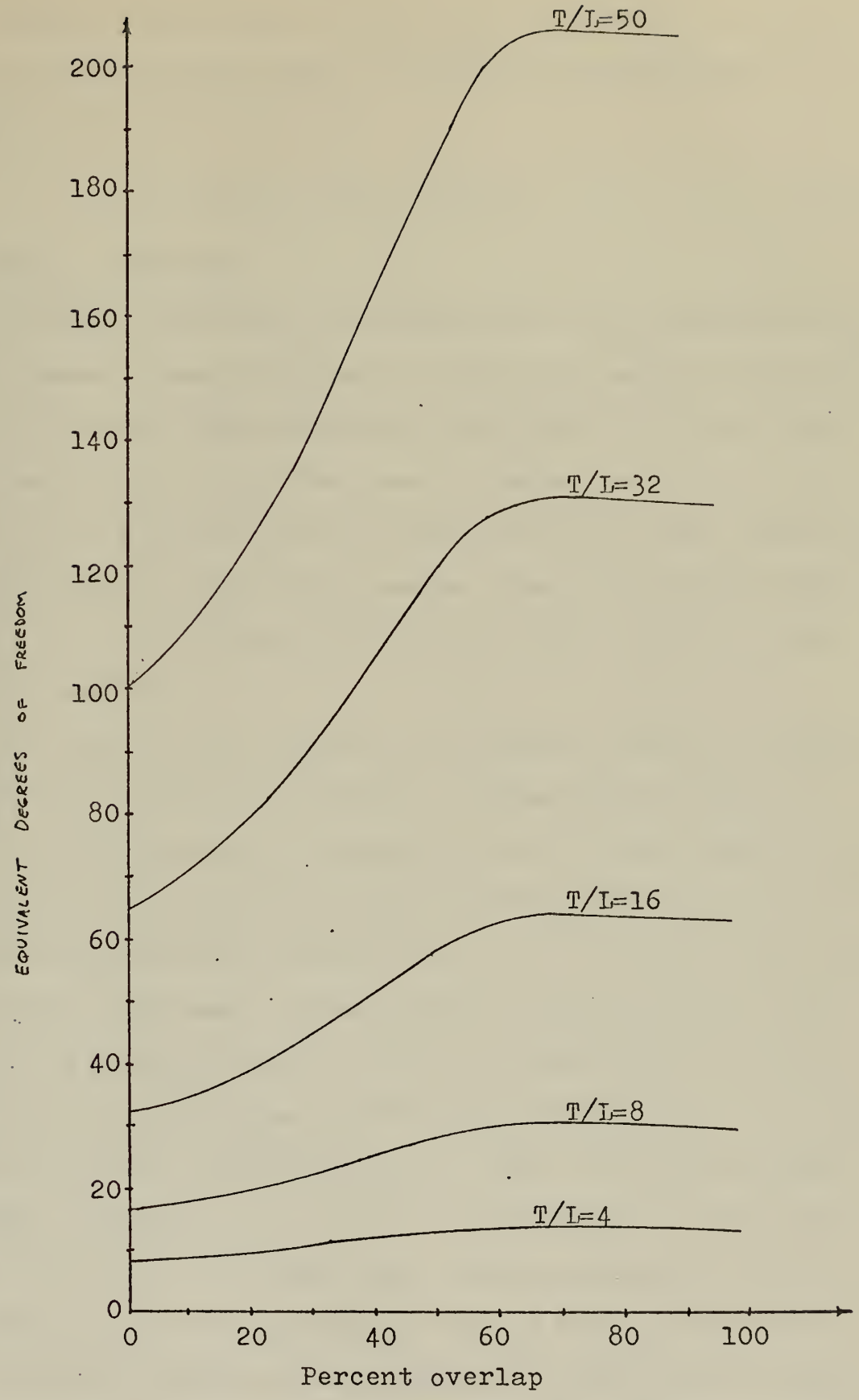

Figure 4.5. EDF vs percent overlap for Hanning window

Usually one would expect N>>T/L, so that the first term of equation will be the most dominant factor in figuring the processing gain. For example, if N = 8192 and T/L = 16,

$$PG = 39.13 + 12.05 = 51.18 \text{ db} \tag{4.54}$$

E. NON-IDEAL CONDITIONS

In the above discussion of processing gain, it was assumed that the signal frequency remained constant over the entire period of observation. If this is not the case, then both PG_T and PG_I will be less than ideal. For example, in the case of the transform, assume that the input frequency is f = j/L for the first N/2 samples and then abruptly jumps to f = (j+1)/L for the remaining N/2 samples. Then, the processing gain (PG_T) for both the j^{th} and $(j+1)^{st}$ filters is N/8, or a loss of 6 db over the ideal case.

Next assume that the frequency is a constant f = j/L for t seconds of the total T seconds of integration, and then abruptly jumps to f = (j+1)/L for the remaining T-t seconds. Then the average power in the j^{th} bin will be attenuated by a factor of t/T and thus PG_I for the j^{th} bin will be attenuated by a factor of t/T (i.e., a loss of 10 $\log_{10}$(t/T) db) from the ideal case. The loss from the ideal case for the $(j+1)^{st}$ bin will be 10 $\log_{10}$ (T-t)/T db. Thus we see that if the integration time is significantly larger than the time the signal spends in the bin, then we can quickly eliminate any gain we might have obtained through the DFT. For example, if T = 256 and t = 80, the loss in the j^{th} bin amounts to 15 db over the ideal case. Careful condideration should therefore be given to the integration time and frequency resolution to to use for the particular problem at hand. Very fine resolution and a long integration time will not aid in detection of a signal which is unstable in frequency and possibly fading in and out besides.

V. SIGNAL DETECTION AND THE HUMAN OPERATOR

A. INTRODUCTION

In the mid-1950's the theory of statistical decision, motivated by problems in radar, was translated into a theory of signal detection. Although the theory specified an ideal process, the generality of the theory suggested that it might also be relevant to the detection of signals by human observers. The relevant theory seemed to provide a framework for a realistic description of the behavior of the human observer in a variety of perceptual tasks. A brief overview of the general theory and a description of certain elements of the signal detection theory appropriate to the human observer are included here to point out the flexibility that a human operator can provide in a signal detection system.

Statistical decision theory specifies the optimal behavior in a situation where one must choose between two alternative statistical hypotheses on the basis of an observed event or series of events. In particular, it specifies the optimal cutoff, along the continuum on which the observed events are arranged, as a function of (a) the a priori probabilities of the two hypotheses, (b) the values and costs associated with the various decision outcomes, and (c) the amount of overlap of the distributions that constitute the hypotheses. In short, the detection problem is a problem in statistical decision; it requires testing statistical hypotheses.

B. FUNDAMENTAL DETECTION PROBLEM

In the fundamental detection problem, an observation is made of events occurring in a fixed interval of time, and a decision is made,

based on this observation, whether the interval contained only the background interference or a signal as well. The interference, which is random, is referred to as noise and is denoted by N; the other alternative is termed signal plus noise and is denoted by SN. In the fundamental problem, only these two alternatives exist — noise is always present, whereas the signal may or may not be present during a specified observation interval. Actually, the observer, who has advance knowledge of the ensemble of signals to be presented, says either "yes, a signal was present" or "no, a signal was not present" following each observation. The fundamental problem will later be extended to include a third alternative - "I'm not sure, continue", but for now consider only the fundamental case.

C. REPRESENTATION OF SENSORY INFORMATION

Any observation may arise, with specific probabilities, either from noise alone or from signal plus noise. This is shown graphically in figure 5.1. The observation is labeled x and plotted on the abscissa. The left-hand distribution, labeled $f_N(x)$, represents the probability density that x will result given the occurrence of noise alone. The right-hand distribution, $f_{SN}(x)$, is the probability density function of x given the occurrence of signal plus noise. Since the observation will tend to be of greater magnitude when a signal is presented, the mean of the SN distribution will be greater than the mean of the N distribution. In general, the greater the amplitude of the signal, the greater will be the separation of these means.

D. OBSERVATION AS A VALUE OF A LIKELIHOOD RATIO

In the discussion thus far it has been assumed that the observation may be represented along a single axis. That this is a valid assump-

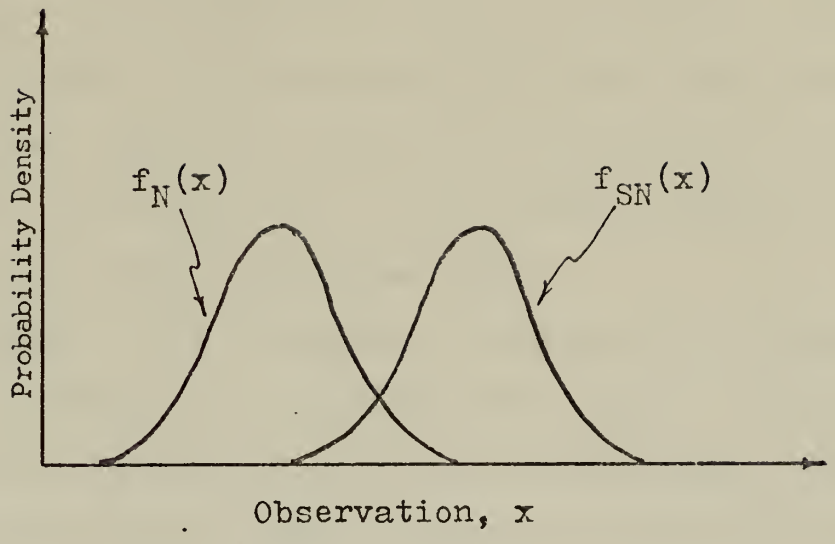

Figure 5.1. The probability density function of noise and signal plus noise.

tion — in spite of the fact that the response of the visual system probably has many dimensions - is explained in terms of some concepts that are basic to the theory.

Assume that the response of the sensory system has several dimensions, and represent it as a point in an m-dimensional space. Call this point y. For each such point in this space there is some probability density that it resulted from noise alone, $f_N(y)$, and similarly some probability density that it was due to signal plus noise, $f_{SN}(y)$. Therefore, there exists a likelihood ratio for each point in the space, $\lambda(y) - f_{SN}(y)/f_N(y)$, expressing the likelihood that the point y arose from SN relative to the likelihood that it arose from N. Since any point in the space, i.e. any sensory datum, may be thus represented as a real, non-zero number, these points may be considered to lie along a single axis. The observation x is thus identified with $\lambda(y)$ and the decision axis becomes the likelihood ratio.

The assumption of a unidimensional decision axis is independent of the characteristics of the signal and noise. Rather, it depends on the fact that just two decision alternatives are considered. More generally, it can be shown that the number of dimensions required to represent the observation is M-1, where M is the number of decision alternatives considered by the observer.

Having established that the observation x may be identified with the likelihood ratio $\lambda(y)$, it can also be shown that we may equally well identify x with any monotonic transformation of $\lambda(y)$; i.e. nothing is lost by distorting the linear continuum as long as order is maintained. In particular, if it is assumed that a transformation of $\lambda(y)$ results in Gaussian density functions on x, the problem will be greatly simplified as will be seen shortly. The existence of such a transformation was

assumed in the representation of the density functions, $f_{SN}(x)$ and $f_N(x)$ in figure 5.1. A further assumption is that the SN function is simply a translation of the N function; i.e., that the two density functions have equal variances. This has been found to be not strictly true, but for the purpose of this discussion the small difference in the variances will not be relevant.

To summarize the last few paragraphs, it has been shown that an observation may be characterized by a value of a likelihood ratio, $\lambda(y)$, i.e., the likelihood that the response of the sensory system y arose from SN relative to the likelihood that it arose from N. This permits viewing the observations as lying along a single axis. It was then assumed that a particular transformation of $\lambda(y)$ would result in normal probability density functions on x. The observer is assumed to base his decisions on the variable x.

E. DEFINITION OF THE CRITERION

From the definition of the problem we see that the observer attempting to detect signals in noise is faced with two alternate hypotheses. He must decide from which hypothesis the observation resulted, N or SN. The observer must establish a policy that defines the circumstances under which the observation will be regarded as resulting from each of the two possible events. He will establish a criterion, a cutoff x_c on the continuum of observations, to which he can relate any given observation x_i. If he finds for the i^{th} observation, x_i, that $x_i > x_c$, he says "SN"; of $x_i < x_c$, he says "N".

The observer's decision will be one of four outcomes: he will say "SN" or "N" and will in either case be right or wrong. The decision outcome, in other words, will be a "hit", a "miss", a "correct rejec-

tion", or a "false alarm". Clearly, these four possibilities are interdependent. For example, an increase in the probability of a hit can be achieved only by accepting an increase in the probability of a false alarm and decrease in the other probabilities. Thus, the balance desired by an observer in any instance will determine the optimal location of his criterion, x_c. The relationship of these four probabilities to one another is shown in figure 5.2, where the probability of a "hit" is represented by region $f_{SN} \cdot A$, the probability of a "miss" by $f_{SN} \cdot B$ (or β), the probability of a "correct rejection" by $f_N \cdot B$, and the probability of a "false alarm" by $f_N \cdot A$ (or α).

There are two conditional probabilities of principal interest. These are the conditional probability of the observer saying "SN" given the occurrence of a signal, $P_{SN}(A)$, and the probability of saying "SN" given the occurrence of noise alone, $P_N(A)$. These two are sufficient since the other two are merely their complements: $P_{SN}(B) = 1 - P_{SN}(A)$ and $P_N(B) = 1 - P_N(A)$. The conditional and joint probabilities are related as follows:

$$P_{SN}(A) = \frac{p(SN \cdot A)}{p(SN)} \tag{5.1}$$

$$P_N(A) = \frac{p(N \cdot A)}{P(N)} \tag{5.2}$$

where $p(SN)$ is the a priori probability of signal occurrence and $p(N) = 1 - p(SN)$ is the a priori probability of occurrence of noise alone. With reference to figure 5.2, note that $P_{SN}(A)$ is the integral of $f_{SN}(x)$ over the critical region A and $P_N(A)$ is the integral of $f_N(x)$ over A.

In statistical decision theory, and in the theory of signal detectability, the optimal criterion for a decision is specified in terms of the

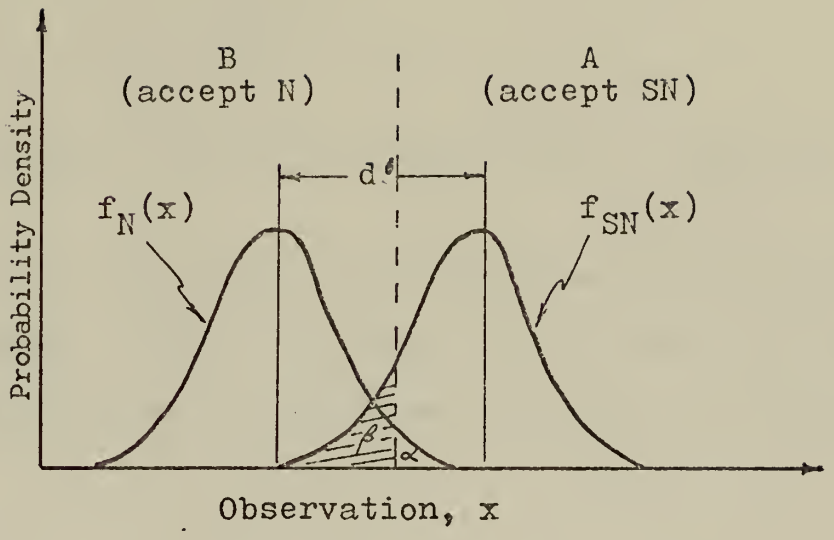

Figure 5.2. The relationship between the four possible outcomes of a simple detection decision.

likelihood ratio. That is to say, it can be shown that the optimal criterion can always be specified by some value θ of $\lambda(x)$. In other words, the critical region A that corresponds to the criterion contains all observations with likelihood ratio greater than or equal to θ, and none of those with likelihood ratio less than θ. To see that this is true, note that the expected value of a decision (denoted EV) is defined in in statistical decision theory as the sum, over the potential outcomes of a decision, of the products of the probability of outcome and desirability of outcome. Thus, using the notation V for positive individual values of the observer and K for costs on negative individual values, we have the following equation:

$$EV = V_{SN \cdot A}\, p(SN \cdot A) + V_{N \cdot B}\, P(N \cdot B) - K_{SN \cdot B}\, p(SN \cdot B) - K_{N \cdot A}\, p(N \cdot A) \qquad (5.3)$$

If a priori and conditional probabilities from equations 5.1 and 5.2 are substituted for the joint probabilites in equation 5.3, then collecting terms yields the results that maximizing EV is equivalent to maximizing

$$P_{SN}(A) - \theta\, P_{N}(A) \qquad (5.4)$$

where

$$\theta = \frac{p(N)}{p(SN)} \cdot \frac{\left(V_{N \cdot B} + K_{N \cdot A}\right)}{\left(V_{SN \cdot A} + K_{SN \cdot B}\right)} \qquad (5.5)$$

It can be shown that this value of θ is equal to the value of the likelihood ratio that corresponds to the optimal criterion. From equation 5.4 it is seen that the value θ simply weights the hits and false alarms and equation 5.5 shows that θ is determined by the a priori probabilities of occurrence of signal and of noise alone and by the values asso-

ciated with the individual decision outcomes. Referring to figure 5.2 and keeping in mind the result that θ is a critical value of $\lambda(x)$, it should be clear that the optimal cutoff x_c along the x axis is at the point on the axis where the ratio of the ordinate value of $f_{SN}(x)$ to the ordinate value of $f_N(x)$ is a certain number, namely θ.

The value of θ above specifies the optimal weighting of hits relative to false alarms; x_c should always be located at the point on the x-axis corresponding to θ. Just where this value of x_c will be with reference to the x-axis depends not only upon the overlap of the two density functions (i.e., upon the signal strength).

F. RECEIVER OPERATING CHARACTERISTICS

Whatever criterion the observer actually uses, even if it is not an optimal criterion, it can be described by a single number — some value of likelihood ratio. By observing how the observer's performance is evaluated with respect to the location of his criterion, it can be seen how his performance may be evaluated with respect to his sensory capabilities.

As previously noted, the fundamental quantities in the evaluation of the operators performance are $p_N(A)$ and $p_{SN}(A)$. Figure 5.3 shows a graph of $p_{SN}(A)$ versus $p_N(A)$, each arc representing a different amount of overlap. Each curve in figure 5.3 corresponds to a given separation between the means of the density functions $f_N(x)$ and $f_{SN}(x)$. The parameter of these curves is labeled d', where d' is defined as the difference between the means of the two density functions expressed in terms of their standard deviation, that is:

$$d' = \frac{\mu_{f_{SN}}(x) - \mu_{f_N}(x)}{\sigma_{f_N}(x)} \qquad (5.6)$$

If the decision criterion is set at the left of figure 5.2, we will obtain a point in the upper right-hand corner of figure 5.3; both $p_{SN}(A)$ and $p_N(A)$ are unity. If the criterion is set at the right end of the decision axis in figure 5.2, a point at the other extreme of figure 5.3 results; both $p_{SN}(A)$ and $p_N(A)$ are equal to zero. Between these two extremes lies the criterion of practical interest. The form of the curves in figure 5.3 is not the only one which might result, but it is the form which will result if the observer chooses a criterion in terms of likelihood ratio, and the probability density functions are normal and of equal variance.

In the context of the detection problem, figure 5.3 is usually referred to as the receiver-operating-characteristic, or ROC curve. The optimal "operating level" is the point on a curve where its slope is equal to θ (see equation 5.5). That is, the expression $p_{SN}(A) - \theta p_N(A)$ defines a utility line of slope , and the point of tangency of this line to the ROC curve is the optimal operating level. Thus the theory specifies the appropriate "hit" probability and "false alarm" probability for any definition of optimum and any set of parameters characterizing the detection situation.

Since the separation between the means of the two density functions is a function of signal amplitude, d' is an index of the detectability of a given signal for a given observer. The variable d' is a measure of the observer's sensory capabilities or the effective signal strength. The criterion that is employed by the observer, which determines the $p_N(A)$ and $p_{SN}(A)$ for some fixed d', reflects the effect of variables which have been variously called the set, attitude, or motives of the observer.

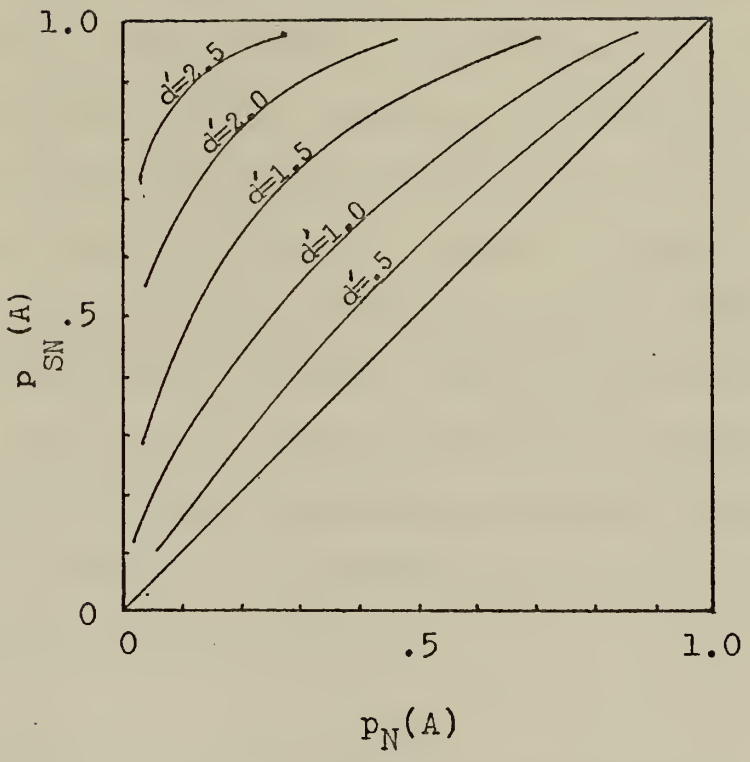

Figure 5.3. Typical ROC curves

G. SEQUENTIAL OBSERVATIONS

If additional observations are allowed before a decision is required, then the observer is assumed to adopt two criteria, or three critical regions. These regions, at least those pertaining to the first observation, are represented as A, B, and C in figure 5.4. If the first observation falls in A the observer says "SN", if it falls in B he says "N", and if it falls in C he says "Continue". The theory of sequential analysis assumes that the successive observations are integrated and that the integrated value is compared with the three critical regions at each observation stage. Thus, a decision is made whenever the combined evidence for one or the other of the two hypotheses is sufficiently persuasive. It is clear that the relationship depicted in figure 5.4 holds only for the first observation in a sequence. A second observation is required only if the first falls in the intermediate region, C. The combination of the first and second observations, therefore, will not be normally distributed , for it results from the addition of a normal variable and a normal variable with both tails missing. Analysis of the inter-relationships of the parameters is extremely difficult in the sequential observation problem because of this.

H. USE OF IDEAL DESCRIPTIONS AS MODELS

At first glance it might appear that a theory of ideal behavior is really not very useful when talking about a human observer. This is not the case, however; ideal behavior constitutes a convenient base from which to explore the complex behavior of a real organism. Ideal conditions generally involve few variables. Having identified the performance to be expected under ideal conditions, it is possible to extend

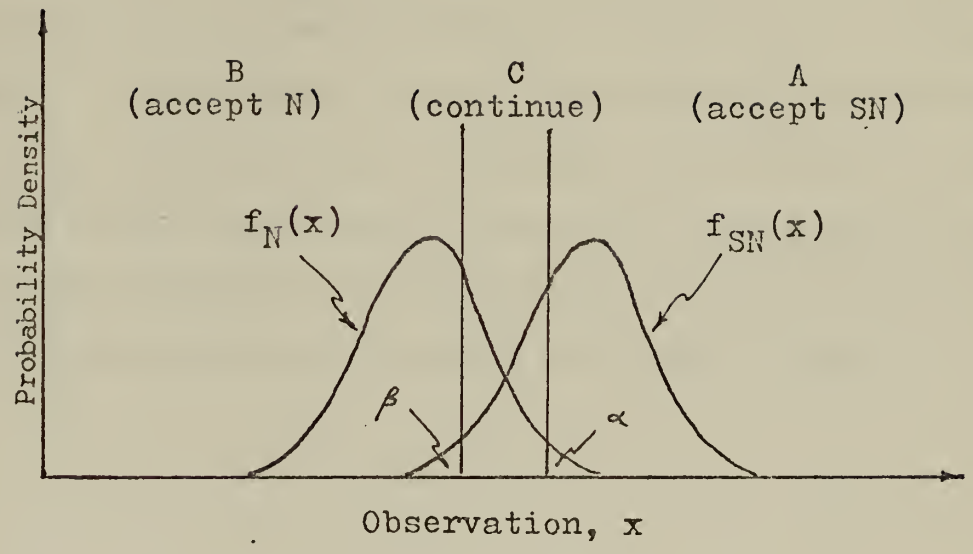

Figure 5.4. Representation of the sequential decision problem.

the model to include additional variables associated with the real world. In studies using human observers in the signal detection problem, it has been found that the ideal theory closely approximates human behavior. The problem is one of altering the ideal model in some way so that it is slightly less than ideal.

The human observer is able to adjust his detection criterion to a particular problem if the information is presented to him in the correct manner. That is, the learning capabilities of the human observer can provide a great deal of flexibility to a signal detection system if he is used correctly. The value of this flexibility will be beneficial however, only if the values of the observer are such that they complement the system. The attitude and motives of the observer play a very important role in the effectiveness of the system. Recent advances in digital processing techniques and computer graphics show great promise in controlling these parameters through increased processor gain and a man-machine interface never before possible with analog equipment.

VI. CONCLUSIONS AND RECOMMENDATIONS

This paper has discussed digital signal processing and spectral analysis techniques as applied to the detection of discrete narrowband signals in a nonstationary noise background. Specifically, the discussion was slanted toward application of a Fourier processor with integration to the Navy's ASW effort. There is a real need today for improved processing techniques and it is apparent that digital processors are the most likely means to improvement. The fast Fourier transform algorithm has led to extensive revision in the methods of frequency domain analysis and real-time digital processors to the point that bandwidths that are sufficient for most problems are a reality today.

It appears that the first attempt at using interactive graphics techniques in the display of a passive ASW signal processor is being made in the "Spotlight" processor. Preliminary use of the display indicates that the operator now has a flexibility and an insight into the detection problem never before possible with previous displays. This particular combination of processing and display has tremendous possibilities in the field of ASW today.

There are two questions fundamental to the ASW detection problem, which the author feels are of primary importance in determining the performance capabilities of a Fourier signal processor such as the "Spotlight" processor. The first is the question of the effects on the spectral estimates of integrating for relatively long periods of time over information which is known to be from a non-stationary background. The second is the human factors question of what is the optimal amount of redundancy required in the display for a processor such as this.

Answers, or at least partial answers, to these questions would aid tremendously in the actual implementation of this type of equipment. Research in these areas is highly recommended since it is only after these questions are answered that the full potential of such a system can be evaluated.

LIST OF REFERENCES

1. Bendat, J. S. and Piersol, A. G., Random Data: Analysis and Measurement Procedures, John Wiley & Sons, Inc., New York, 1971.

2. Blackman R. B. and Tukey J. W., The Measurement of Power Spectra, Dover Publications, Inc., New York, 1958.

3. Enochson, L. D. and Otnes, R. K., Programming and Analysis for Digital Time Series Data, The Shock and Vibration Information Center, Naval Research Laboratory, Washington D.C., 1968.

4. Jenkins, G. M. and Watts, G. G., Spectral Analysis and Its Applications, Houghton-Day Company, San Francisco, 1968.

5. Nuttall, A. H., Spectral Estimation by Means of Overlapped FFT Processing of Windowed Data, Naval Underwater Systems Center Report No. 4169, 1971.

6. Parkins, B. E., Studies on Time Variation of Ambient Sea Noise and Scattering of Acoustic Signals From Rough Surfaces, Bell Laboratories, Inc., Whippany, N. J., TR No. 23, 1968.

7. Pryor, C. N., Calculation of the Minimum Detectable Signal for Practical Spectrum Analysers, Naval Ordinance Lab., White Oak, Silver Spring, Maryland, NOLTR 71-92, 1971.

8. Pryor, C. N., Effect of Finite Sampling Rates on Smoothing the Output of a Square Law Detection With Narrow Band Input, Naval Ordinance Lab., White Oak, Silver Spring, Maryland, NOLTR 71-29, 1971.

9. Rabiner, L. R. and Rader, C. m., Digital Signal Processing, IEEE Press, 1972.

10. Swets, J. A., Signal Detection and Recognition by Human Operators, John Wiley & Sons, Inc., New York, 1964.

11. Taub, H. and Schilling, D. L., Principles of Communication System, McGraw-Hill Book Company, New York, 1971.

12. Thomas, J. B., and Ricker, G., Statistical Communication Theory, John Wiley & Sons, Inc., New York, 1969.

13. Williams, J. R. and Ricker, G., Signal Detectability Performance of Optimal Fourier Receivers, Interstate Electronics Corporation, Anaheim, California, IEC Technical Note 4800-600, 1972.

INITIAL DISTRIBUTION LIST

		No. Copies
1.	Defense Documentation Center Cameron Station Alexandria, Virginia 22314	2
2.	Library, Code 0212 Naval Postgraduate School Monterey, California 93940	2
3.	Professor G. A. Rahe Department of Electrical Engineering Naval Postgraduate School Monterey, California 93940	12
4.	LT. Vance E. Adler, USN 22704 Picador Dr. Salinas, California 93901	1
5.	Professor D. M. Powers Department of Electrical Engineering Naval Postgraduate School Monterey, California 93940	1
6.	Chairman Department of Aeronautics Naval Postgraduate Shool Monterey, California 93940	1

REPORT DOCUMENTATION PAGE

READ INSTRUCTIONS BEFORE COMPLETING FORM

1. REPORT NUMBER

2. GOVT ACCESSION NO.

3. RECIPIENT'S CATALOG NUMBER

4. TITLE (and Subtitle)

Digital Processing of Acoustic Signals With Application to an ASW Signal Processor

5. TYPE OF REPORT & PERIOD COVERED

Master's Thesis; December 1973

6. PERFORMING ORG. REPORT NUMBER

7. AUTHOR(s)

Vance Erick Adler

8. CONTRACT OR GRANT NUMBER(s)

9. PERFORMING ORGANIZATION NAME AND ADDRESS

Naval Postgraduate School
Monterey, California 93940

10. PROGRAM ELEMENT, PROJECT, TASK AREA & WORK UNIT NUMBERS

11. CONTROLLING OFFICE NAME AND ADDRESS

Naval Postgraduate School
Monterey, California 93940

12. REPORT DATE

December 1973

13. NUMBER OF PAGES

14. MONITORING AGENCY NAME & ADDRESS (if different from Controlling Office)

Naval Postgraduate School
Monterey, California 93940

15. SECURITY CLASS. (of this report)

Unclassified

15a. DECLASSIFICATION/DOWNGRADING SCHEDULE

16. DISTRIBUTION STATEMENT (of this Report)

Approved for public release; distribution unlimited.

17. DISTRIBUTION STATEMENT (of the abstract entered in Block 20, if different from Report)

18. SUPPLEMENTARY NOTES

19. KEY WORDS (Continue on reverse side if necessary and identify by block number)

Signal Detection
Signal Processing
Digital Signal Processing
ASW Signal Processing
Fast Fourier Transform
Discrete Fourier Transform
Spectral Analysis
Hanning Window
Acoustic Analysis

20. ABSTRACT (Continue on reverse side if necessary and identify by block number)

There is a growing need within the Navy for methods of detecting discrete narrowband signals in a non-stationary background. This paper concerns itself with the application of digital processing and spectral analysis techniques toward that goal. The use of the fast Fourier Transform in estimating the power spectrum of a signal is described. The method involves sectioning the time record, making "raw" estimates of the spectrum from

these sections, and averaging these "raw" estimates. It is shown that more stable estimates are available if the segments are overlapped and an optimum amount of overlap for the case of the Hanning window is found. It is shown that the stability of these spectral estimates can be interpreted as processing gain in the case of a discrete narrowband signal in additive noise. And finally, a brief description of signal detection theory applied to a human observer is presented to emphasize the flexibility that a human operator can bring to a signal detection system.

Thesis
A254
c.1

147694

Adler

Digital processing of acoustic signals with application to an ASW signal processor.